DNMI
Det norske meteorologiske institutt

Spatial interpolation of temperatures in Norway applying a geostatistical model and GIS.

REPORT NR.26/98

Ole Einar Tveito & Eirik J. Førland

KLIMA

DNMI-REPORT

NORWEGIAN METEOROLOGICAL INSTITUTE
P.O. BOX 43 BLINDERN, N - 0313 OSLO
TELEPHONE: (+47) 22 96 30 00

ISBN 0805-9918

REPORT NO.
26/98 KLIMA

DATE:
16.10.98

TITLE:

Spatial interpolation of temperatures in Norway applying a geostatistical model and GIS.

AUTHORS:

Ole Einar Tveito & Eirik J. Førland

PROJECT CONTRACTORS:

Norwegian Electricity Federation (EnFO), (contract no. 55108)

Norwegian Meteorological Institute

SUMMARY:

In this study, a geostatistical approach for spatial interpolation of Norwegian mean monthly air temperature normals has been applied. Air temperature is regarded as a product of two components, a deterministic and a stochastic component. The temperature lapse rate is used as a deterministic component describing the temperature variations with altitude. The temperatures are reduced to sea level applying the lapse rate, and a geostatistical model is used to describe the spatial variation of the residuals.

Analysis is carried out both at station level and sea level using different lapse rates. Cross-validation shows enhanced results applying residual kriging. Generally very good estimated are obtained, but a few large estimation errors occur, especially during the winter months. These problems are connected to the lapse rate, which is influenced by local inversions and föhn-effects.

The approach presented in this report is an objective and consistent method for mapping temperature, and is a major step forward in intergrating GIS and automatic mapping procedures within climatological analysis.

SIGNATURES:

Eirik J. Førland

Eirik J. Førland
PROJECT COORDINATOR

Bjørn Aune
HEAD OF DIVISION

Contents

1. Introduction

Knowledge about the spatial variation of climatological elements is of major interest for a wide group of users. Such information is used in both the planning and operation of different installations influenced by climatological conditions. They may be input variables to hydrological models, both for energy production and water supply management. Climatology is also an important factor to consider in the design of installations such as dams, roads, bridges, power lines, tele-towers etc. which may be affected by extreme weather conditions, leading to a safety risk or economic loss. Very often, such installations are situated at locations without meteorological. It is therefore one of the challenges within climatology to estimate the climate at locations without measurements.

Despite the complexity of the factors affecting the local climate, the traditional way of describing the spatial variability of different climate elements has, from a methodical point of view been quite simple. They have been manual methods, regional averages, nearest neighbour or weighted averages (like Thiessen polygons). During the recent years, computer capacity as well as digital archives of climate data have increased, and made it possible to apply more sophisticated approaches within this field. Especially the introduction of Geographical Information Systems (GIS) has made it possible in an easy way to combine different types of spatial distributed data which may describe the climatological variations.

The present investigation was initiated by the project "Regionalisation of climate statistics" supported by the Norwegian Water System Management Association (EnFO). The objective of this investigation is to develop methods for confident estimation of climate statistics for both points without observations as well as areal values. Temperature is chosen as pilot parameter in this study. There are two reasons why the temperature is examined first:

- Temperature varies relatively smooth, and the variations are explained by physically based principles. It is therefore simpler to model than more randomly distributed parameters like precipitation. For the development of new methodology, temperature is more easy to understand than other climatological elements, e.g. precipitation.

- Temperature is a key element in distributed snowaccumulation and snowmelt models, and better representation of temperatures in different altitude zones is of great interest for production planning and operation of river regulations. This is also a safety precaution in case of possible floods due to snow melt.

In this report, application of a geostatistical approach is described. Factors influencing the spatial distribution of air temperature is discussed in section 2, while section 3 gives a breif review of geostatistical principles for spatial interpolation. In the next sections, a description of data and the analysis of monthly normal temperatures are presented and discussed. In the last sections, uncertainties in the estimates are evaluated.

2. Factors affecting the spatial distribution of air temperature

2.1 Lapse rate and føhn-effects

The climatological conditions in Norway show a large spatial variation. Southern Norway belongs to (at least) seven climate zones based on Köppens macro-climate classification scheme (Johannessen, 1977). In the coastal areas the climate is maritime, with small amplitudes both in diurnal, seasonal and annual temperature amplitudes. Eastern parts however experience a more continental climate with large temperature amplitudes. This is an effect of both large-scale circulation, radiation budget and local terrain effects.

The local climate depends for it general characteristics upon the regional climate and ultimately upon the global climate system. The mechanisms acting to create a local climate are essentially the same as those creating the global climate. The most vital considerations are the character of the surface and how it varies spatially and interacts with the overlying atmosphere.

The atmosphere is transporting heat from the tropics to the polar regions, with the sun as heat source. The air temperature may be high in areas with high net radiation balance, but also the surface characteristics play an important role for the temperature in the boundary layers. E.g. the surface layers of the ocean may heat during day and cool during night with a daily temperature amplitude of less than 1°C. The meteorological conditions being the same, the daily temperature amplitude over dry sand may exceed 50 °C.

As an average the temperature in the troposphere decreases by 0.65 °C per 100 m increase in altitude. This lapse rate is reflecting the difference between the average global surface temperature, ~15 °C and the average temperature at the tropospause (-59 °C at ca. 11 km altitude). (74 °C/~11000 m = ~0.673 °C/100m). There are however large variations around this mean temperature lapse rate, especially in the lowest part of the troposphere. But also at higher elevations the lapse rate may vary substantially in time and space. In dry air the lapse rate is ca. -1.0 °C/100m. In humid (saturated) air latent heat is released during condensation. This release of latent heat, - and thus also the lapse rate, varies with altitude in saturated air. In the lower and middle part of the troposphere the lapse rate is approximately -0.5 °C/100m. When saturated air is lifted over a mountain range the temperature at the (humid) windward side will decrease by ca 0.5 °C/100m. If the condensated water is precipitated on the windward side, the (dry) air will be warmed by 1.0 °C/100 m by subsidence on the leeward side. In situations with this so-called *føhn-effect* the lower-lying areas on the leeward side of a mountain range will get higher temperatures than areas in the same elevation at the windward side. An example (05.02.1990) is shown in Figure 2.1.

Bruun (1957) studied the lapse rate for a number of pairs of Norwegian stations and divided them into groups based on the degree of ventilation in the area. The number of pairs were limited to avoid the problem of the horizontal temperature gradient. Bruun (1957) states that the global lapse rate of -0.65°C/100m was not representative for monthly, seasonal or annual mean temperatures in Norway. The vertical gradient varies with season and location. She defined four groups of stations, having different vertical

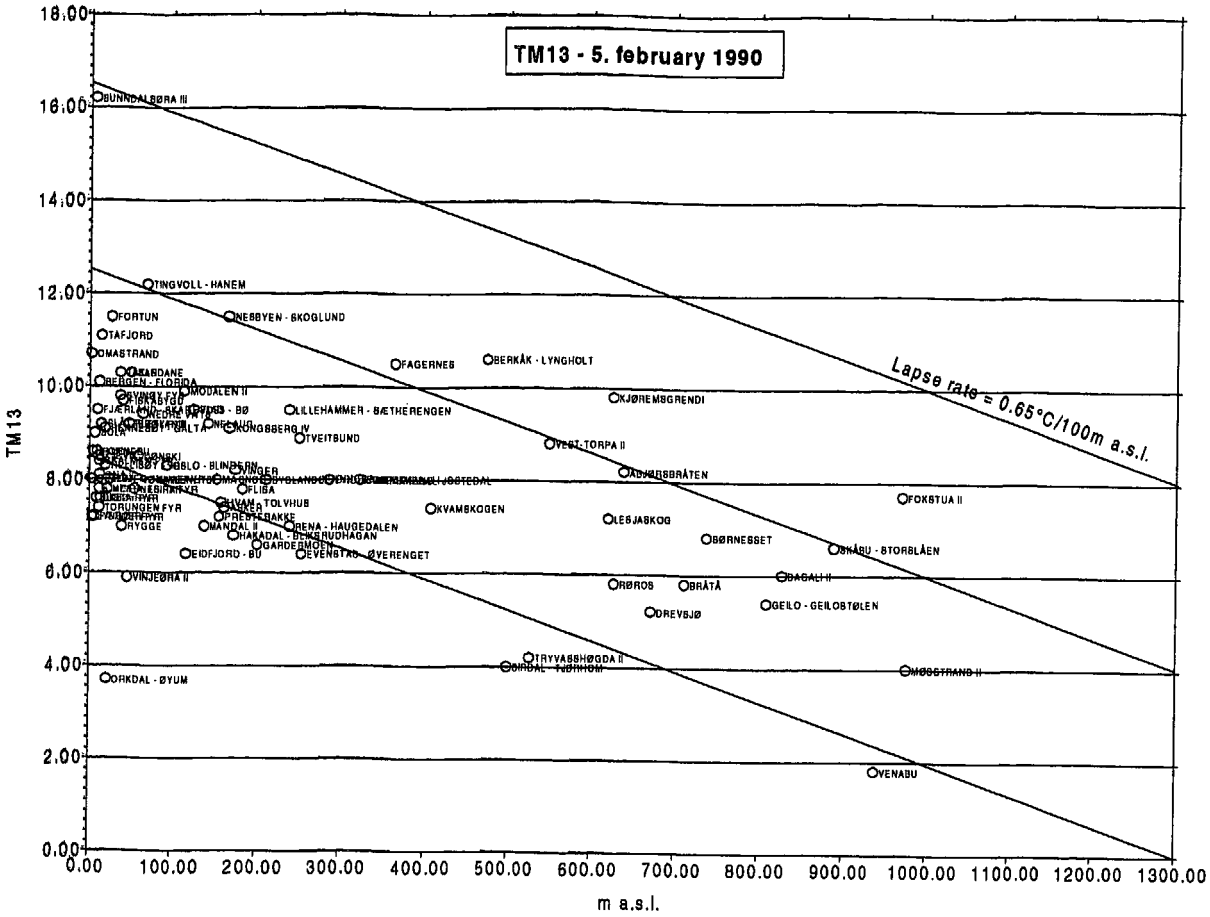

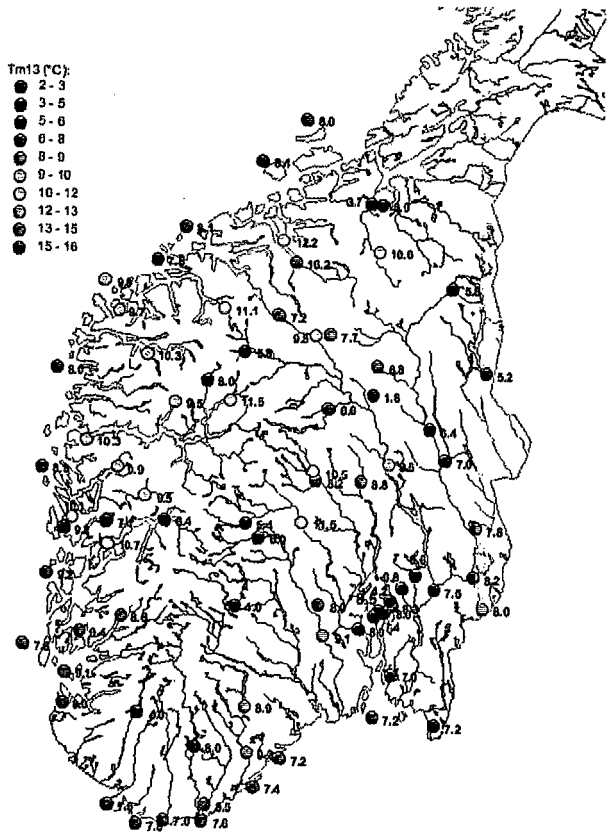

Figure 2.1 Temperature distribution during a föhn-situation.

gradients:

A. Well ventilated stations, small terrain variations.
B. Well ventilated stations, large terrain variations.
C. Valley stations, small terrain variations.
D. Coastal stations.

Group C can be divided into two groups, having moderate cold depressions or deep cold depressions. Based on pairs of observations classified into these groups, Bruun (1957) established mean vertical temperature gradients, shown in table 2.1. Tveito (1998) has revealed similar gradients for southern Norway applying linear regression analysis. These are also shown in table 2.1. The gradients are largest in spring and autumn, and smallest in winter and summer. This is explained climatologically by the presence of inversions, as they are more likely to be present in winter and summer than in spring and autumn. Bruun (1957) found the vertical gradient to vary throughout the year, with the smallest lapse rate in the winter (typical values -0.3 - -0.4°C/100 m a.s.l.). At some well protected locations, the gradient even appeared to be positive (temperature increase with altitude), an effect of temperature inversions. The highest lapse rates were found in spring and autumn (typical values -0.7°C/100 m a.s.l.). This was the case for all the groups, but the variance in lapse rate is larger at protected locations compared to locations which are well ventilated.

Table 2.1 Vertical temperature gradients (°C/100 m) at Norwegian stations (Bruun (1957), Tveito (1998)).

		Number of pairs	Jan	Feb	Mar	Apr	May	Jun	Jul	Aug	Sep	Oct	Nov	Dec	Year
Bruun (1957)	Group A	2	-0.42	-0.52	-0.69	-0.82	-0.82	-0.82	-0.69	-0.75	-0.73	-0.76	-0.60	-0.52	-0.70
	Group B	4	-0.36	-0.38	-0.48	-0.61	-0.70	-0.71	-0.69	-0.63	-0.61	-0.55	-0.47	-0.37	-0.55
	Average of A and B	-	-0.38	-0.42	-0.54	-0.68	-0.74	-0.74	-0.69	-0.67	-0.64	-0.62	-0.51	-0.42	-0.60
	Group C_1	3	+0.16	-0.07	-0.27	-0.56	-0.64	-0.58	-0.52	-0.44	-0.39	-0.30	-0.11	+0.18	-0.30
	Group C_2	5	+0.62	+0.29	-0.12	-0.46	-0.63	-0.57	-0.54	-0.44	-0.30	-0.20	+0.10	+0.50	-0.14
	Group D	1	-0.68	-0.74	-0.74	-0.74	-0.70	-0.68	-0.62	-0.70	-0.70	-0.66	-0.68	-0.68	-0.70
Tveito(1998)	Southern Norway	226 stations	-0.30	-0.33	-0.54	-0.67	-0.67	-0.62	-0.59	-0.56	-0.54	-0.47	-0.41	-0.32	

2.2 Inversions

It is important to notice that the tropospheric lapse rate of -0.65 °C/100 m is an average value and that the actual lapse rate may differ substantially from this value both in time and space. During nights with clear skies and calm wind conditions, hollows and valley floors act as reservoirs for cold air. The surface is cooled by longwave radiation, and the cooled air in the lowest boundary layers are more dense than the surrounding air. This cold air will consequently sink down against the lowest lying parts of the terrain where it will be still further cooled. Under such weather conditions (*inversions*) the air temperature will increase with altitude in the lower part of the atmosphere. In stable clear weather periods during winter, the surface inversion may be several hundred meters thick. Figure 2.2. shows the variation of surface temperature both vertically and horizontally in such a situation.

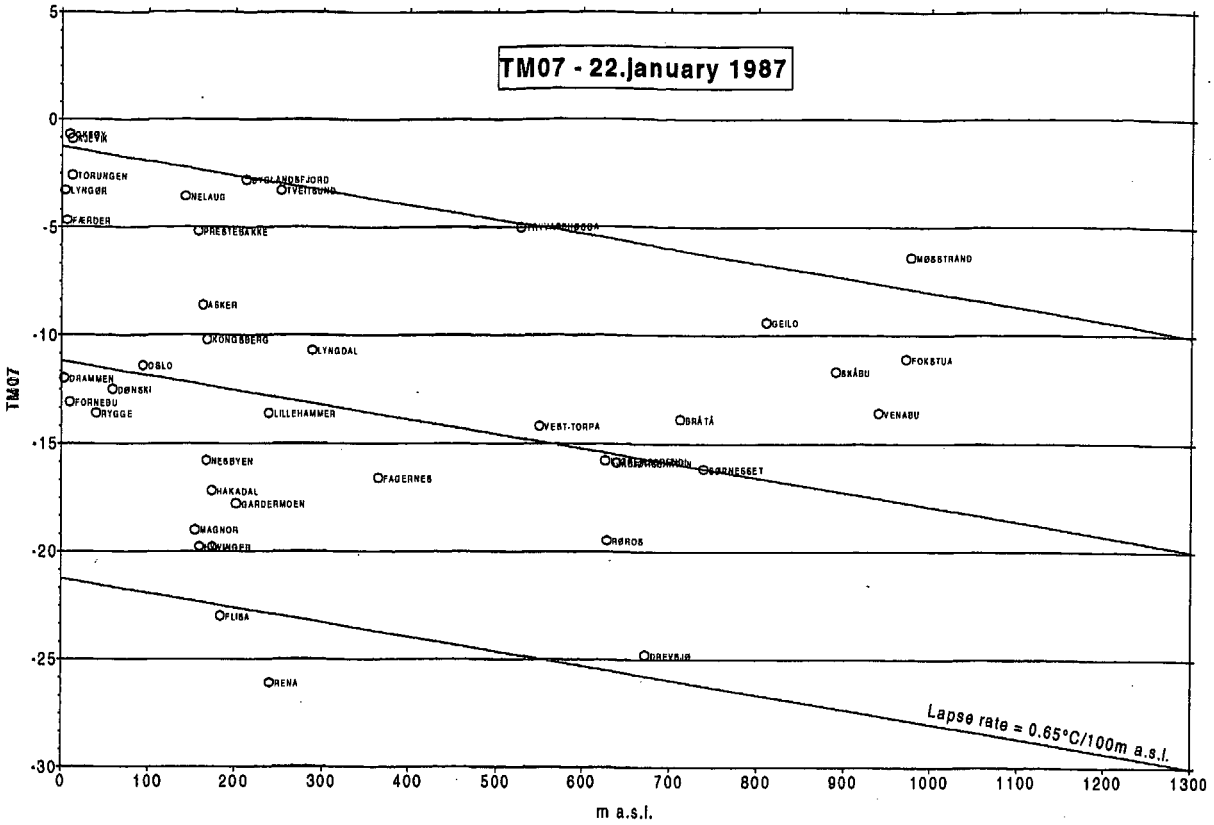

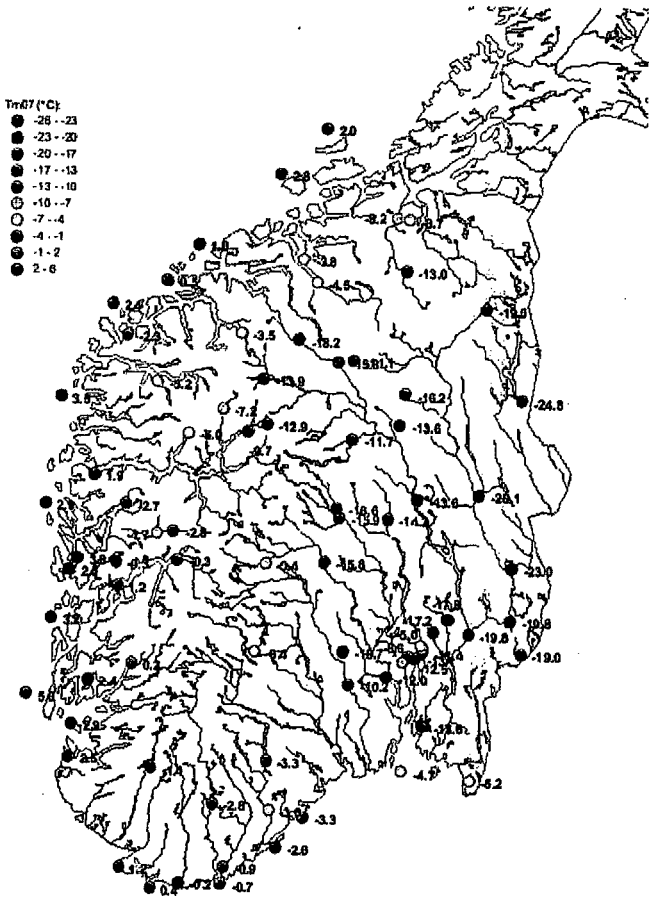

Figure 2.2 Temperature distribution in an inversion situation

On the other hand, in mid-summer the warming during daytime may be significantly higher in such hollows/valleys than in the surrounding terrain, because these low-lying areas may be sheltered from wind.

Contrary to hollows and valleys, hilltops and mountains are characterised by a more smoothed temperature climate. The heating of the surface is levelled off at such more wind exposed sites. The heated air in the boundary layer over a hill side can during daytime be effectively mixed with cooler air from the free atmosphere. During night the cooled air close to the ground will stream down the hillside, and be replaced by warmer air from the surrounding free atmosphere.

Also wind conditions play an important role for the local air temperature. During weather situations with short-wave insolation and calm the air in the surface layer will be warmed substantially. With increasing wind, turbulence will mix the warm surface air with cooler air from higher levels in the atmosphere. Also inversions may be broken down by increasing wind, as the cold air then will be mixed with warmer air from aloft. During high wind speeds such inversion layers will not be formed. The diurnal temperature range and the local temperature gradients are thus larger in periods with calm than during windy conditions (Førland and Skartveit, 1979).

The climatology at the Nes-peninsula (16 × 10 km) in the Lake Mjøsa was studied by Utaaker (1963). He used a dense station network, and even observed temperature profiles from a running car. Analysis of minimum temperatures in weather situations with inversions showed differences up to 8-9 °C over short distances. This particular difference was observed at two stations approximately 3 km apart, with an elevation difference of 170 m, giving a vertical temperature gradient 5.3 °C/ 100 m a.s.l. Also in an area with elevation differences less than 100 m (Lysaker-Slependen, near Oslo), Aune and Førland (1987) found local temperature differences of 8-9 °C over short distances during inversion conditions in January-February 1987.

2.3 Advection and dependence on distance from the coast

In addition to the local radiation balance, the local temperature conditions are strongly dependent on advection. Advection is taking place on a number of different scales, from macro to micro scale. The global «westerlies» generally advects airmasses from west-south-west towards Scandinavia. During wintertime this dominating wind direction is coming from areas with relatively high surface temperature, and is the main cause of the relatively high winter-temperatures in Scandinavia. While the global mean temperature along 60 °N in January is -17 °C, the western coast of Denmark, southern Norway and Sweden has a mean temperature of about 0 °C. Along 70 °N the mean temperature in January is -27 °C, while Hammerfest at the same latitude has -4 °C.

In advective weather situations the airmasses will be influenced by the energy balance in the underlying areas. The air temperature will thus vary with the distance from the coast. By using a two-parameter linear regression model Førland (1984) found that the mean

winter temperature in Western Norway decreased by 0.6 °C per 100m increase in altitude, and simultaneously decreased by 0.03 °C per km increase of distance from coast.

In his studies in the Nes-area (Utaaker, 1963) found substantially smaller local spatial variation in maximum than in minimum temperatures. The largest difference in mean maximum temperature between the stations was 1.5 °C. For some single days, the local differences in maximum temperature was up to 4 °C. Utaaker (1963) concluded that much of the local variability of temperature is explained by exposition and the nearness to the Lake Mjøsa.

2.4 Modelling the spatial distribution of air temperature

Both Carrega (1995) and Zheng and Basher (1996) applied similar approaches as Førland (1984). In their study of New Zealand temperature normals, Zheng and Basher (1996) used a relationship:

$$T = f(e^{-DTC})$$

where DTC is distance to coast.

Tveito (1998) has described the spatial variability of the 1961-90 monthly temperature normals for southern Norway applying multiple linear regression. Altitude and distance to coast were used as independent variables. The regression coefficients of the two independent variables showed a seasonal variability, and the altitude coefficient showed similar response as indicated by Bruun (1957). Reasonable good models describing the monthly means were found. However, a global method like regression will fail in some areas of a large, inhomogeneous area, but will probably work better in smaller and more homogenous regions.

Because of the maritime influence, the distance to the coast is expected, in addition to altitude, to have significance for temperature estimation. Consequently, it may be assumed that :

$$T = f(Z, DTC)$$

where T is mean monthly temperature normal, Z is altitude and DTC is distance to coast.

3. Methods for spatial interpolation

3.1 Stochastic and deterministic temperature components.

The spatial variation of temperature is a function of several processes. As described in chapter 2, the vertical temperature gradient and distance from coast are components that may be described as deterministic terms. However, the process will have local variations which are more random, and may be described as stochastic processes. Following this philosophy, temperature can be expressed as:

$$T = T_D + T_S + \varepsilon$$

where T_D is the deterministic (trend) component of the temperature, T_S is the stochastic part and ε is the residual (which is not explained by the deterministic or stochastic components). The components can be splitted into several sub-models, both deterministic and stochastic:

$$T_D = T_{D_1} + T_{D_2} + T_{D_3} + \ldots\ldots\ldots + T_{D_n}$$

and

$$T_S = T_{S_1} + T_{S_2} + T_{S_3} + \ldots\ldots\ldots T_{S_n}$$

In the interpolation approach used in this study the deterministic components of air-temperature are removed, and the remaining temperature field is examined by spatial statistical methods.

The large-scale determinstic component of air temperature (i.e. the part described by lapse rate and distance to coast), is strongly influenced by local conditions. It is therefore difficult to find a confident algorithm to classify the local temperature gradients. Consequently the global mean lapse rate of -0.65 °C/100 m and the average gradient by Tveito (1998) is applied. The anomalies in the remaining temperature field is then examined, partly using geostatistics.

3.2 Objective interpolation and kriging

Objective analysis (optimum interpolation) is a term introduced by Gandin (1963), and is frequently used within applied climatology. The approach introduced by Gandin is however not widely used within climatological statistics, mostly because it is based on correlations between data series, and thereby demands several realisations of the process, i.e. time series of climatic elements.

Kriging is another approach based on the same statistical principle. It is a widely used interpolation method in cases were only one or a few realisations of the process to be interpolated are available. It was developed for geological problems, but has been successfully used also in other disciplines.

Kriging is a linear interpolation method, which can be formulated:

$$X^*(\mathbf{u}_0) = \sum_{i=1}^{n} \lambda_i X(\mathbf{u}_i)$$

where λ_i is the interpolation weight of the value $X(\mathbf{u}_i)$, i is the index of the station, $\mathbf{u}$ is the co-ordinate vector and n is the number of observations used in the interpolation. The interpolation weights in an ordinary kriging system are estimated by:

$$\sum_{j=1}^{n} \lambda_j(\mathbf{u}_0) C(\mathbf{u}_j - \mathbf{u}_i) + \mu(\mathbf{u}_0) = C(\mathbf{u}_0 - \mathbf{u}_i), \qquad i = 1, \ldots\ldots, n$$

$$\sum_{j=1}^{n} \lambda_j(\mathbf{u}_0) = 1$$

The interpolation weights are dependent upon the spatial model $C(\mathbf{u}_j\text{-}\mathbf{u}_i)$. In kriging the spatial model, the semivariogram, is defined as:

$$\gamma(\mathbf{h}) = \frac{1}{2N(\mathbf{h})} \sum_{i=1}^{N(\mathbf{h})} (X(\mathbf{u}) - X(\mathbf{u}+\mathbf{h}))^2$$

where $\mathbf{u}$ is the location vector and $\mathbf{h}$ is a distance vector. $N(\mathbf{h})$ is the number of pairs within the distance lag.

This equation calculates the experimental semivariogram, based upon the observations. Then an empirical model is adapted to this semivariogram. Kriging is an exact interpolation method. Observed values will always be returned when interpolating to a point. When interpolating to a grid cell, the interpolated value is the average over the points in the grid cell, and may therefore deviate from observed points within the cell. The size of the deviation depends on the variability of the element within the gridcell. If the grid cell is inhomogoneous, e.g. in topography, deviations in the estimate of temperature may be considerable.

3.2.1 Statistical assumption for the semivariogram

As for most statistical methods, the application of spatial variance models assumes that the process has an underlying statistical distribution. A regional dataset is said to be stationary if all the moments at all locations are the same. This criterion will however hardly ever be fulfilled, so a criterion of second order stationarity has to be defined. The process have the same mean value, and the spatial variance is a function of distance between the observations points only. Mathematically this can be expressed as:

$$E[X(U) - X(u+h)] = 0 \qquad \text{Stationarity of 1. order.}$$

$$Var\{X(u) - X(u+h)\} = f(h) \qquad \text{Stationarity of 2. order.}$$

which leads to the variance model:

$$f(h) = \mathrm{var}\{X(u) - X(u+h)\} = 2\gamma(h)$$
$$\gamma(h) = C(o) - C(h), \quad \forall \mathbf{u}$$
$$C(0) = \mathrm{var}\{Z(u)\}, \quad \textbf{stationary variance}$$

3.2.2 Semivariogram models

The model fitted to the experimental semivariogram has at least two parameters (sill and range), sometimes three (also the nugget effect). The parameters are:

- Sill - which is the maximum γ(h)-value. It describes the variance explained by the model.
- Range - which describes the distance of influence of the model.
- Nugget effect - describe the discontinuity close to zero distance, and is used when the variogram value not approaches 0 when $h \rightarrow 0$. This parameter often describes the uncertainty of the measurements, or lack of spatial representativity.

The most used semivariogram models are:

Spherical model:

$$\gamma(h) = \begin{cases} c_0 + c \cdot \left[\frac{3}{2} \cdot \frac{h}{a} - \frac{1}{2} \cdot \left(\frac{h}{a} \right)^3 \right], & \text{if } h \leq a \\ c_0, \quad , & \text{if } h \geq a \end{cases}$$

Exponential model:

$$\gamma(h) = c_0 + c \cdot \left[1 - e^{-\frac{h}{a}} \right]$$

where a is the range, h is the distance and c is the sill. c_0 is the nugget effect.

3.3 Anisotropy

Application of kriging and the semivariogram models assume the co-variation to be the same in all directions. If this is not the case, the process is regarded as anisotropic. Then the interpolation should be carried out such as the process is treated as isotropic. This can be done in two ways:

- put constraints on the semivariogram, so that the range is different in different directions.
- make a co-ordinate transformation of the input points so they are projected into an isotropic field.

In this paper, the first approach is applied.

3.4 Crossvalidation

Crossvalidation is a procedure of testing the chosen estimation model. It works as a loop running through all the observation points. For each loop one of the locations is temporarily removed from the dataset, and a value for this location is estimated from the other observations in the data set. Using such a procedure is objective and almost independent[1]. Cross-validation gives both estimation statistics and «true» estimation errors at each location in the datasample.

4.Description of climatological conditions and data sample

4.1 Climatological conditions

The study area for this analysis is southern Norway. The area is mountainous, with large variations in climate over short distances. The west coast is dominated by humid westerly winds from the Atlantic. At the coast, the terrain rises up to 1000-2000 meters in just a few kilometres. Otherwise the terrain is dominated by long and deep fjords. This give high precipitation values, the mean annual precipitation is above 1500 mm (max. 3575mm) in large parts of Western Norway. As the ocean acts like a temperature conservator, the temperature variation in the coastal areas throughout the year is quite small.

A high mountain area runs all the way from the south and northwards (Figure 4.1), with altitudes above 1000 m a.s.l. East of the mountain range the climate is continental, with cold winters and warm summers. The temperature range between absolute annual maximum and minimum temperatures can in some places exceed 70°C (-35°C - + 35°C). The terrain is dominated by large valleys. In these valleys inversions are frequent during winter time. The precipitation is generally low, less than 1000 mm/year.

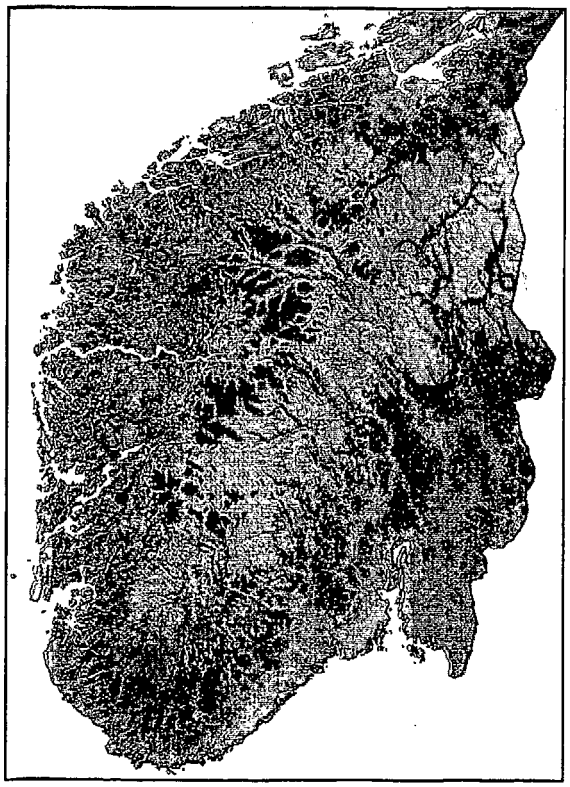

Figure 4.1 Topographical map of the analysis area.

The eastern part is protected by the mountains, and wind conditions are

[1]Almost independent means that the location is included in the sample used for the estimation of the semivariogram. It is independent in the calculation of the interpolation weights λ and the interpolation itself.

calm. The climate is continental, and the temperature conditions are often dominated by the local radiation balance, resulting in cold winter and/or warm summer temperatures.

4.2 Data sample

The data used in this investigation is the official Norwegian monthly mean temperatures 1961-90 (Aune, 1992). For southern Norway, temperature normals are calculated for 232 meteorological stations. Stations with observation periods less than 10 years were removed from the data set. To be able to perform a completely independent verification of the estimation, a few more stations were randomly withdrawn from the dataset. This resulted in a final dataset of 156 temperature stations used in the analysis.

5.Spatial analysis at station level

Normal values (1961-90) for the 156 temperature stations in Southern Norway were analysed. Special attention was made to the spatial variability. Each month were examined separately.

5.1 Semivariograms

Semivariograms for the mean monthly temperature normals (1961-90) in southern Norway were calculated using the GSLIB software (Deutsch and Journel, 1992). The semivariograms reveal large differences between the different months and seasons. Distance lag for the semivariograms are 10 km, and a full circle search was used. Anisotropy was not evaluated at this stage of the investigation.

The semivariogram for annual mean values is shown in Figure 5.1. There are large variations between the different distance lags. The variance of the annual values is 6.44. The variograms for the individual months are shown in Figures 5.2-5.4, grouped by seasons.

The winter season (Figure 5.2) shows the largest variability, and the lowest variability is found for the summer months (Figure 5.4). For distances shorter than 275 km all the variograms show the same major patterns, but for larger distances, the summer months have another variation than the other months. This is an effect of the warm continental climate of central eastern Norway in the summer. In the other seasons this area is colder than the coastal and mountain areas.

The winter semivariogram shows larger variability at shorter distance lag, e.g. at distances between 75 and 140 km. One remarkable feature is the local minima at 80, 140 and 210 km for all semivariograms. The almost constant distance interval between these minimas

should be investigated further.

The high variability, with peaks and lows in the semivariogram may indicate that anisotropy is present. If this effect is present it will however be an effect of altitude and continentality.

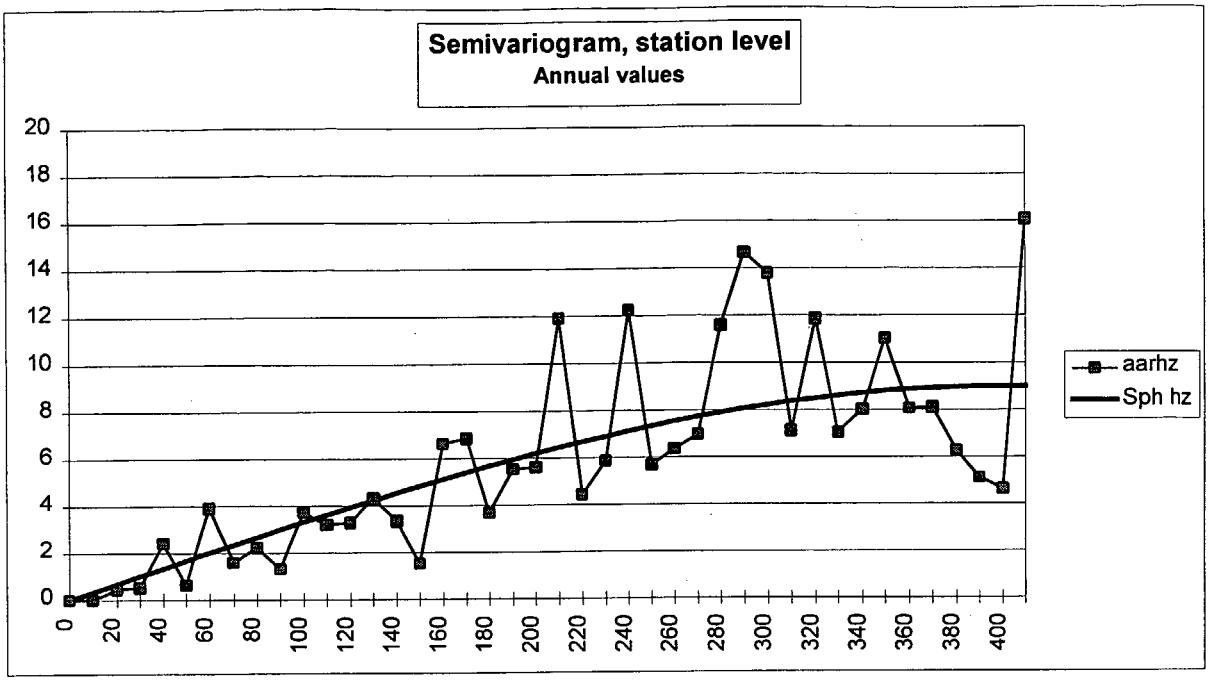

Figure 5.1: Semivariograms at station level, annual mean temperature.

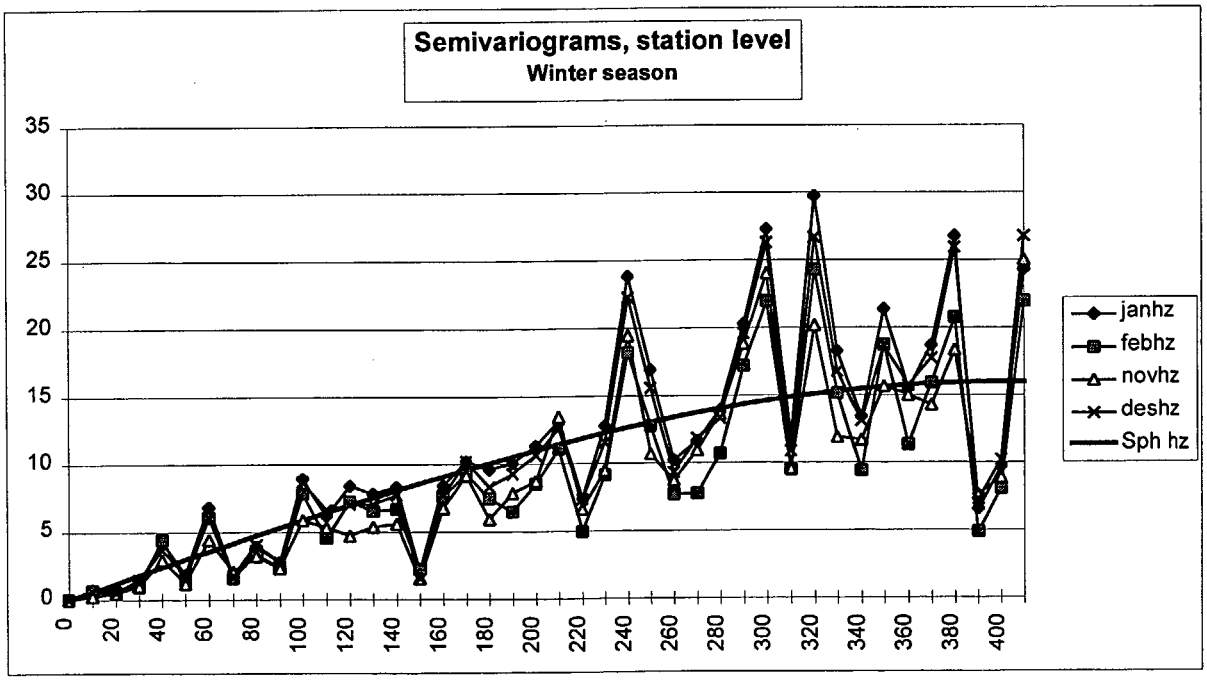

Figure 5.2: Semivariograms at station level, winter season.

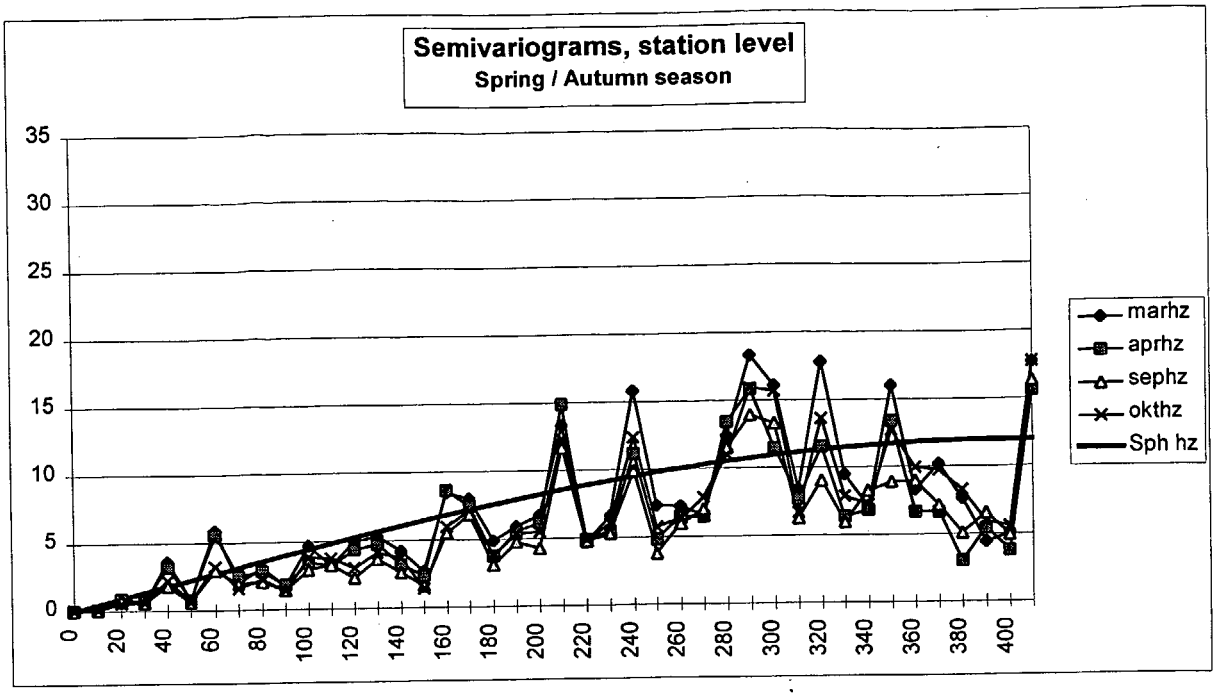

Figure 5.3 Semivariograms at station level, spring and autumn months.

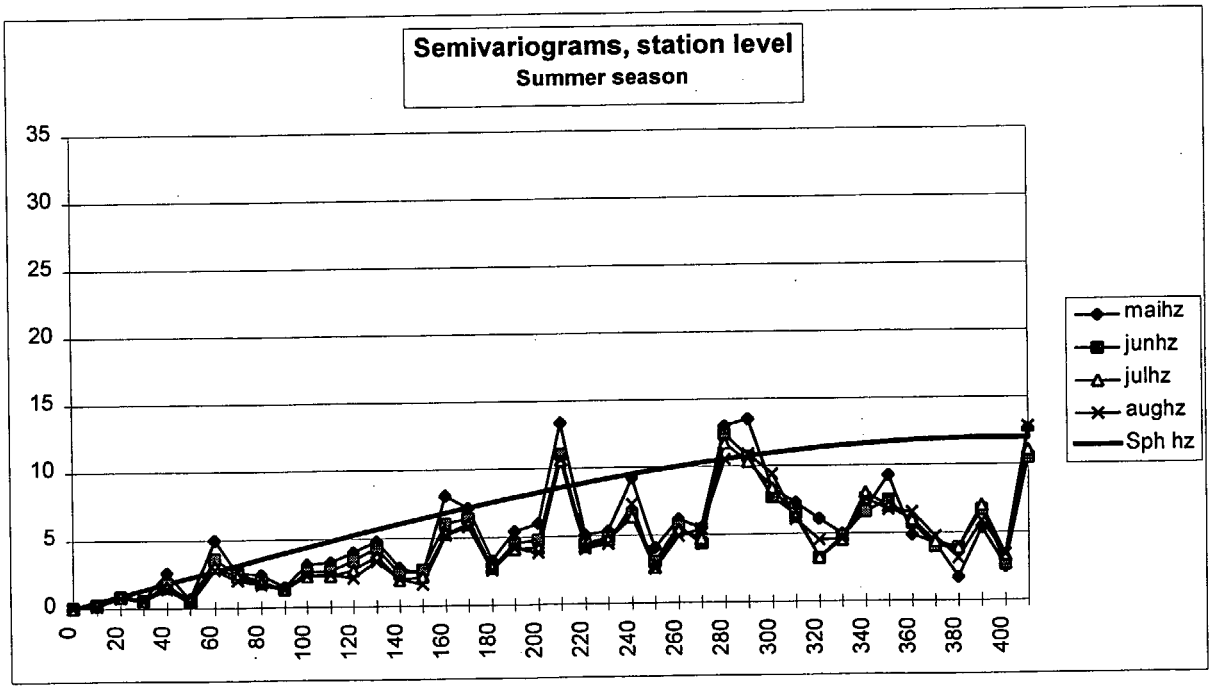

Figure 5.4 Semivariograms at station level, summer months.

5.2 Semivariogram models

Spherical models are fitted to the observed semivariograms. Typical range for the variograms are 300-400 km, shortest for the summer months (300 km, Figure 5.4) and longest (400 km) for the others. The sill is lowest in the summer, higher in the spring and autumn and very high in the winter season. The fitted semivariogram values are shown in table 5.1.

Table 5.1: Semivariogram (spherical) parameters at station level.

Season	*Sill*	*Range*
Winter	16	400 km
Spring/Autumn	12	400 km
Summer	6.5	300 km
Annual	9	400 km

5.3 Crossvalidation

Temperature estimates are evaluated by crossvalidation. The semivariogram models in table 5.1 are used.

Crossvalidation shows large errors in the estimated temperatures in both January and April, which are the two months given most attention. The errors in January (Figure 5.5) are varying between 4 °C underestimation and 6 °C overestimation. Generally, the smallest errors are found in the coastal areas, the largest in inland areas with strong relief. The main reason for these errors are the large vertical temperature anomalies, which are not taken fully into account in the statistical model. The largest errors are found at stations in and near deep valleys and deep fjords.

In April (Figure 5.6) the number of stations which are estimated satisfactorily is higher. There are however a number of locations where the model gives large errors. These errors occur mainly at station in and near the high mountain district in central southern Norway. There is also a valley - mountain difference in over- or underestimation, which is not surprisingly, since the nearest station will have the highest loadings in the linear interpolation equation. This station is not necessarily the «nearest» station climatologically speaking. In springtime, when the snow has melted away in the lowland, it can still be present at higher altitude levels. This difference in surface characteristics may also lead to temperature anomalies not covered by the statistical interpolation model.

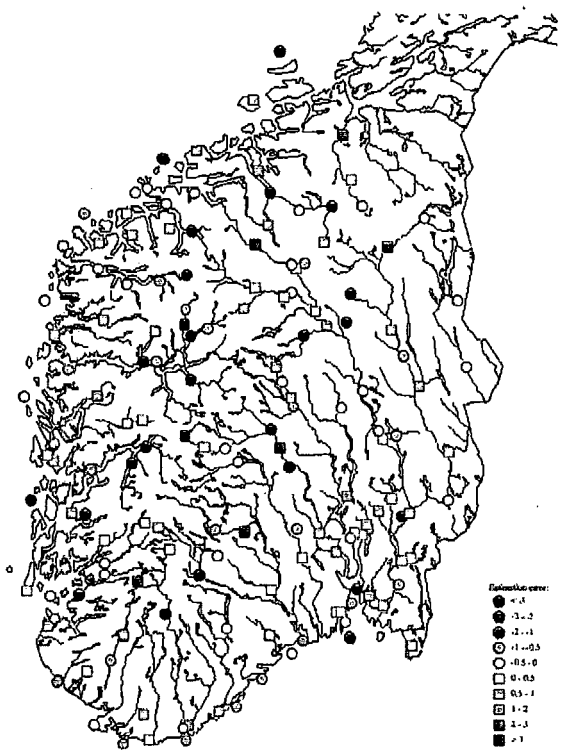

Figure 5.5 Crossvalidation at station level, January.

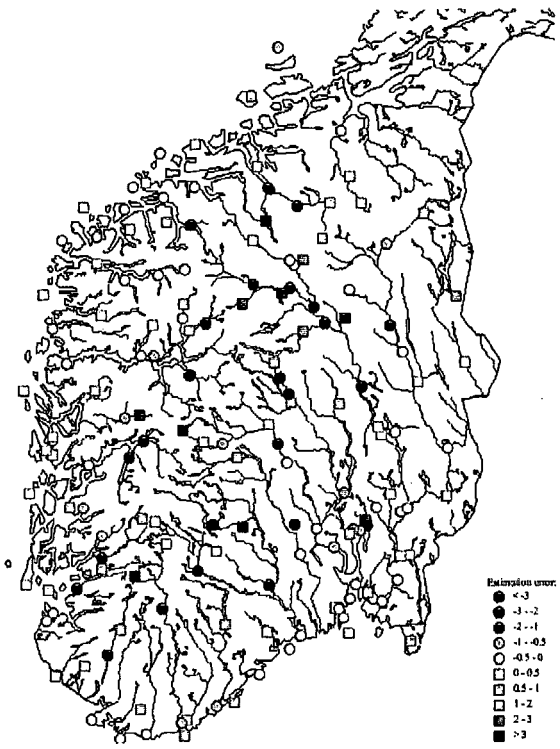

Figure 5.6 Crossvalidation at station level, April.

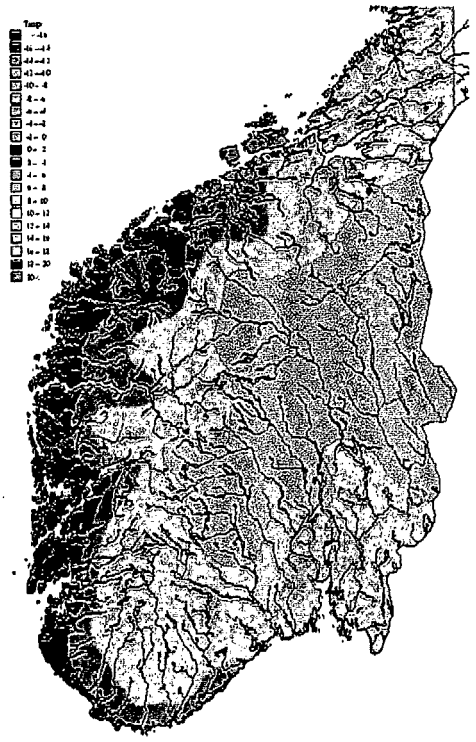

Figure 5.7 Temperatures interpolated at station level, January.

Figure 5.7 Temperatures interpolated at station level, April.

5.4 Maps

Temperature maps for the two months are estimated using the statistical model presented in table 5.1. The maps are shown in Figure 5.7 (January) and Figure 5.8 (April). They shows the general temperature variations as smooth surface where the topographical influence is suppressed. Some stations which deviates from the general regional patterns, e.g. observations at mountain peaks or extreme inversions, will cause temperature peaks or sinks in the map. Such an effect is created by the station Gaustadtoppen (No. 31970, see appendix A) in both maps. This station is situated on an isolated mountain peak 1828 m a.s.l., and is representing free atmosphere conditions.

5.5 Comments on station level estimation

The analysis of temperature at station level does not take topographical variation into account, and therefore suppresses the large variations in temperature that occur due to terrain variations. The maps produced by the station level approach cannot be used for further climatological analysis. An approach including terrain variations should therefore be applied.

6.Spatial analysis at sea level

As presented in the previous chapter and in chapter 2.2, the global lapse rate of -0.65 °C/100m can be used as a rough description of temperature as a function of altitude. In this investigation all the monthly and annual mean values was reduced to sea level using this constant vertical temperature gradient and the gradients found by Tveito (1998). The gradients by Tveito (1998) show a seasonal variation.

6.1 Semivariograms, constant lapse rate.

The semivariograms of the temperatures reduced to sea level applying the constant lapse rate -0.65°C/100m for all the months is shown in Figures 6.1-6.3. The seasonal behaviour in these variograms are not as pronounced as in the station level variograms. The winter season (Figure 6.1) shows a very large variance compared to the other months. November has another behaviour than the other months in this group, with less variance. The range is almost the same for these months, around 150 km.

In the summer (Figure 6.3) there is a separation between June and July, and May and August. The two midsummer months have larger variability and no defined range. May and August have less variability, but also these two months are without a clearly defined range.

In spring and autumn (Figure 6.2) there is also different behaviour. March and October have much of the same characteristics, however larger variability for March at short distance lags. April has very little variance, September have almost the same behaviour as March for about 225 km, then the variance increases. It is however possible to use a semivariogram model with range <100 km for these months.

In the present paper January and April is investigated, using a spherical semivariogram model with the parameters presented in table 6.1.

Table 6.1: Semivariogram (spherical) parameters at sea level.

Season	*Sill*	*Range*
January	5.0	150 km
April	0.4	75 km
October	0.4	75 km

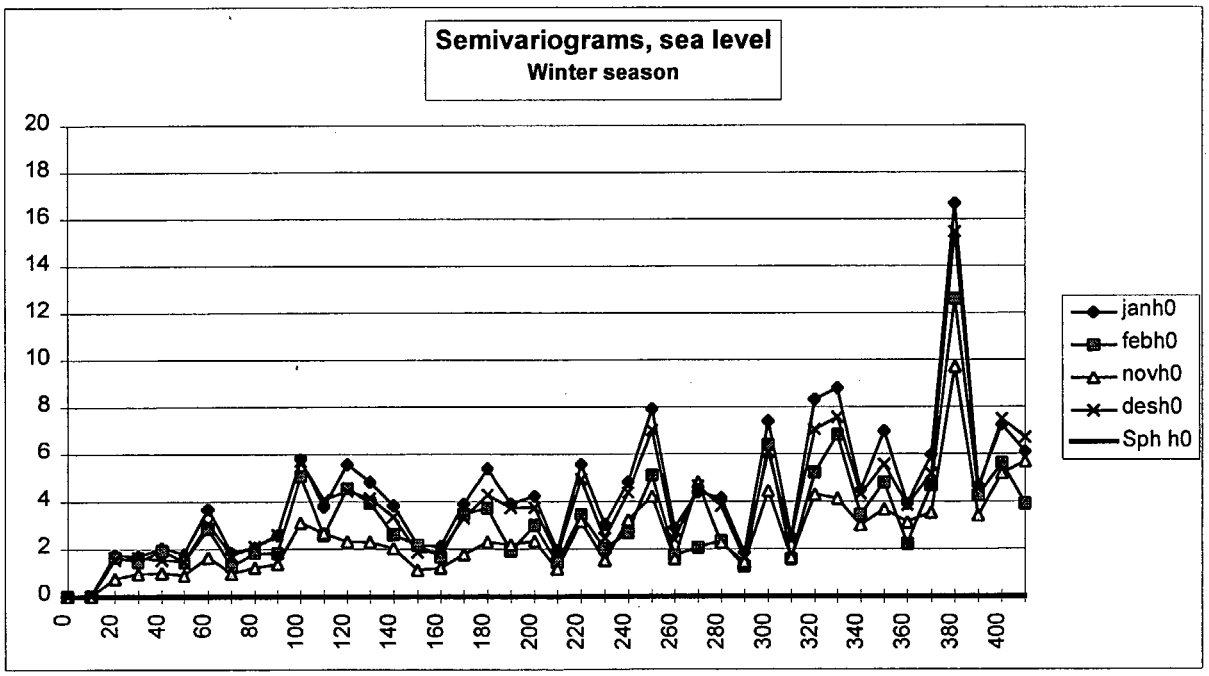

Figure 6.1: Semivariograms at sea level, winter months.

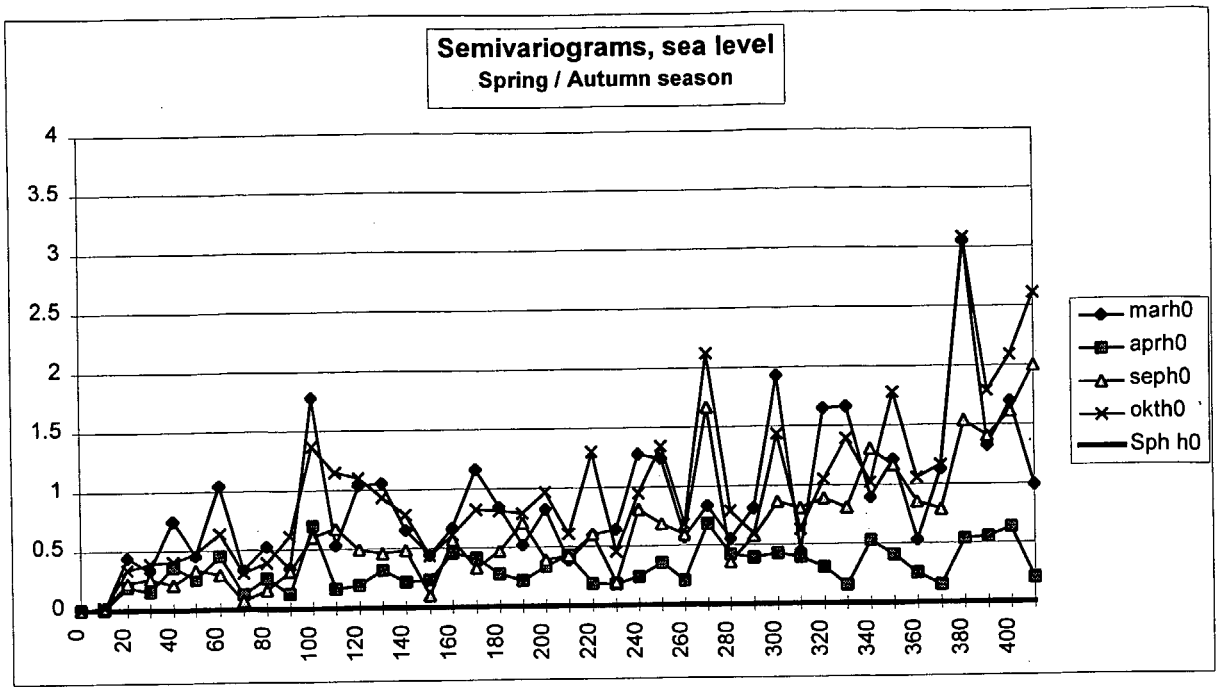

Figure 6.2: Semivariograms at sea level, spring-autumn months.

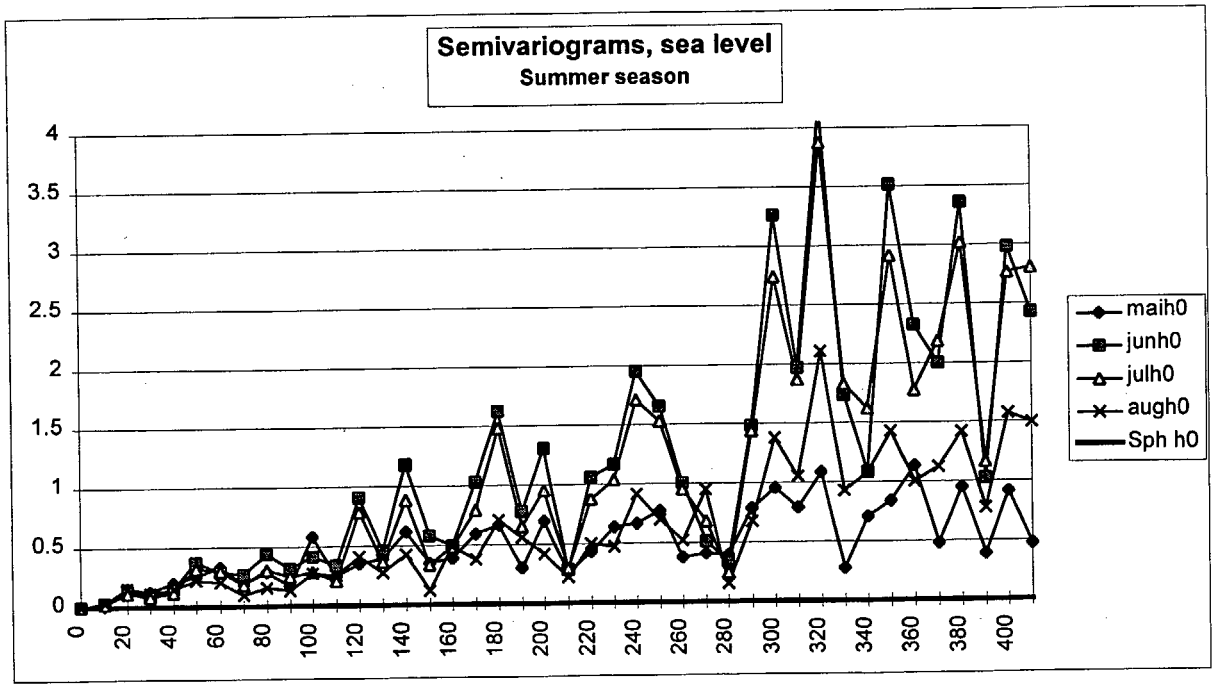

Figure 6.3: Semivariogram values at sea level, summer months.

6.2 Crossvalidation

The results of the crossvalidation is presented as maps in Figures 6.4 (January) and 6.5 (April).

For January there is not any improvement in estimating temperature at sea level compared to estimation at station level. The main reason is probably that inversions cause large local difference in the lapse rate. At some locations it seems as the estimation error is strengthened in some way, as if the reduction to the sea level emphasises the vertical temperature variations. The estimates are generally poorer at locations where there are large differences in station altitude between neighbouring stations.

In April the estimates are improved compared to the estimates based on station level data. Only six stations have errors larger than 1°C. Most of these locations are in bottom of fjords (underestimation) or in high mountain areas (overestimation).

6.3 Maps

Making maps using the reduced temperature data is a two step process. First a map at sea level is calculated by kriging using the semivariogram model. Thereafter this map is combined with the digital elevation model (Figure 4.1) to calculate temperatures at terrain level.

The January map at sea level is shown in Figure 6.6. This map shows large variations from the west coast and eastwards. At the west coast the temperatures are positive, up to 3 °C. In the interior continental parts the temperature goes down to -10 °C. Some «islands» occur, due to deviating stations. These islands are inversion stations (in the large valleys) and mountain peaks (Gaustadtoppen). The map in Figure 6.6 is combined with the digital elevation model using the formula:

$$TM_Z = TM_{H0} - 0.0065 \cdot Z$$

where TM_Z is the temperature in terrain level, TM_{H0} is the temperature at sea level and Z the digital elevation model. The resulting fine resolution (1×1 km) map is presented in Figure 6.7. This map is much more detailed than the station level map, including topographical variability. It is also much more detailed than the manually drawn maps (Aune, 1993).

The April map at sea level is shown in Figure 6.8. This map shows very little spatial variation, and the temperature range is 2.9 - 6.0 °C. The map shows some colder areas around areas with glaciers and in the north-east part of the mapped area. The resulting map at terrain level is shown in Figure 6.9.

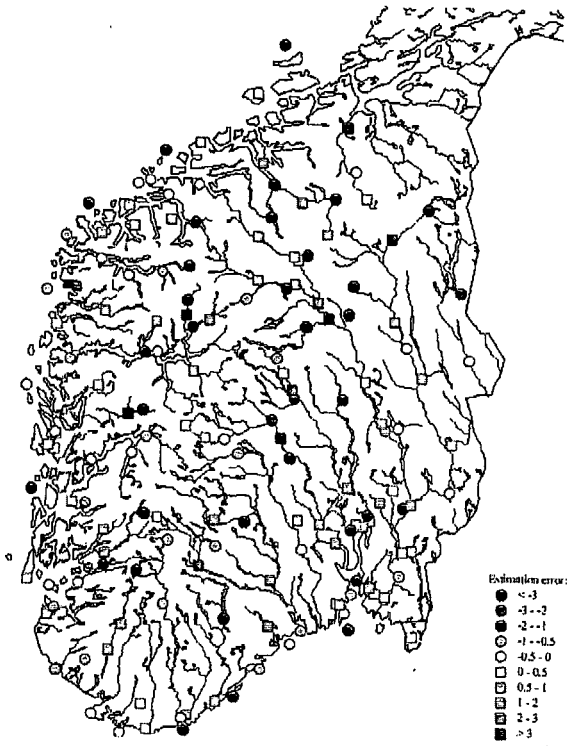

Figure 6.4 Crossvalidation at sea level (constant lapse rate), January.

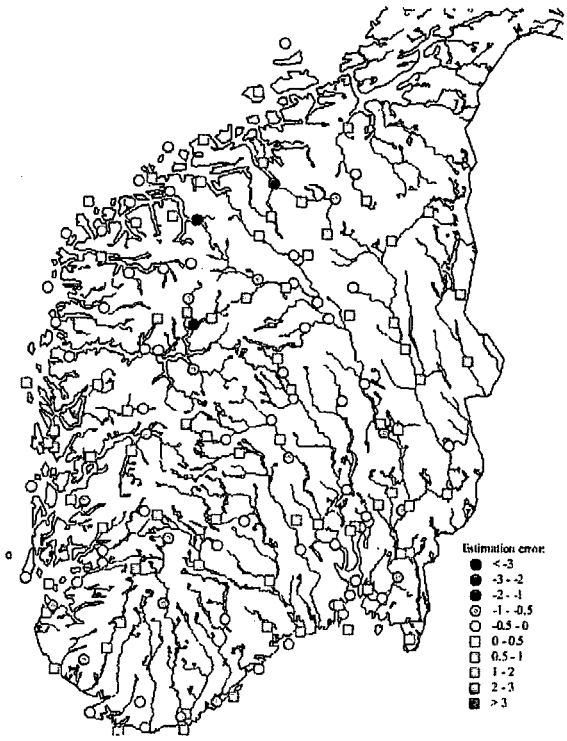

Figure 6.5 Crossvalidation at sea level (constant lapse rate), April.

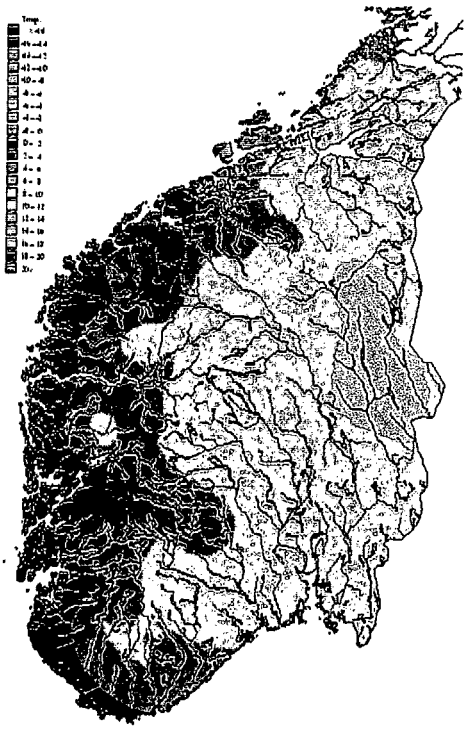

Figure 6.6 Interpolated temperatures at sea level (constant lapse rate), January.

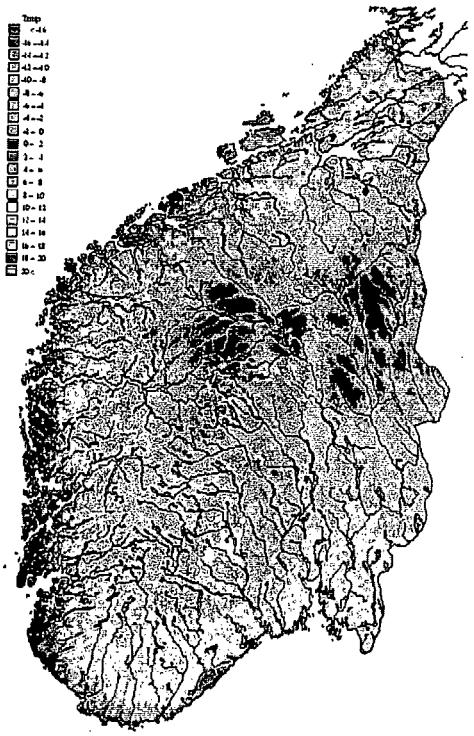

Figure 6.7 Interpolated temperature at terrain level (constant lapse rate), January.

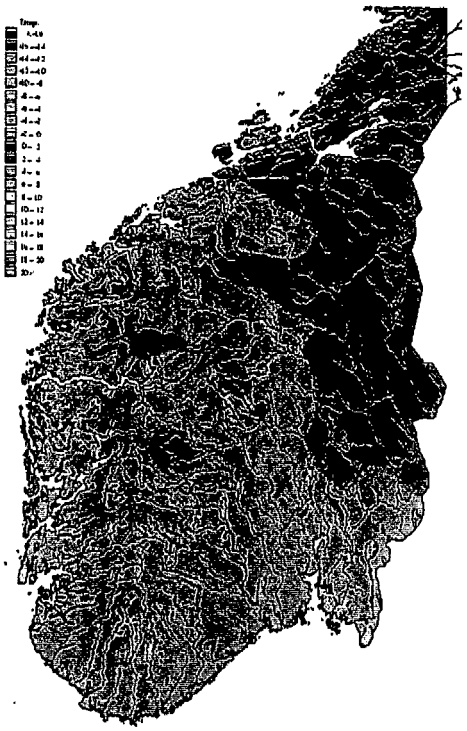

Figure 6.8 Interpolated temperature at sea level (constant lapse rate), April.

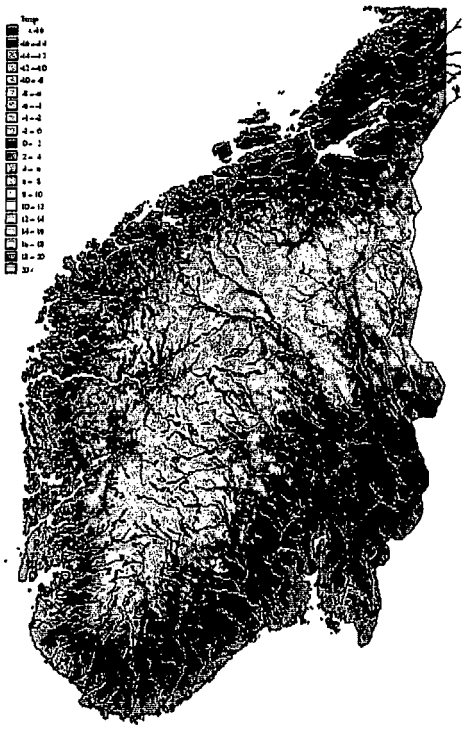

Figure 6.9 Interpolated temperature at terrain level (constant lapse rate), April.

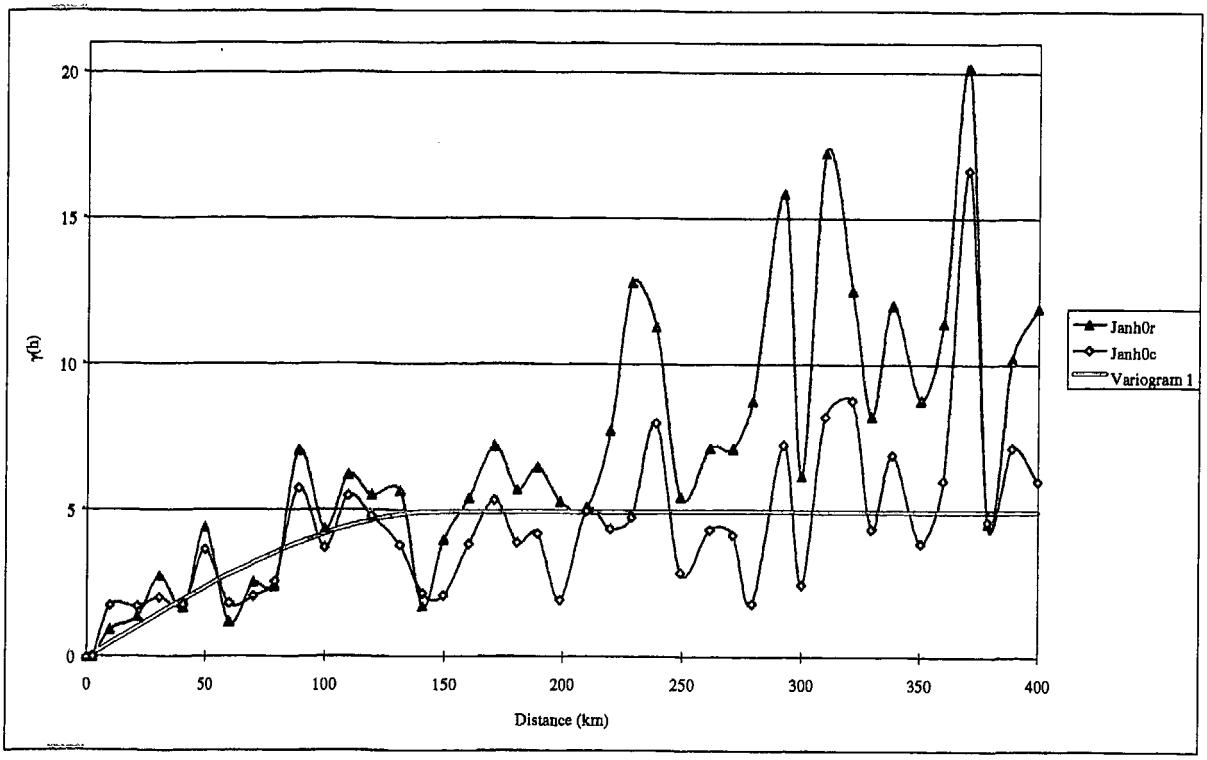

Figure 6.10 Semivariogram, seasonal (janh0r) vs. constant (janh0c) lapse rate, January.

6.4 Semivariograms applying a seasonal lapse rate

Tveito (1998) showed that the vertical temperature gradient has a seasonal variation in Southern Norway. The monthly gradients established by applying linear regression are listed in table 2.1.

The difference between the constant and the seasonal gradient is largest in January, mostly due to the frequent occurrence of inversions at that time of the year. The difference is generally large during the winter season, while it is small during the other seasons.

Here an example applying the seasonal gradient for January is presented. The observed temperatures are reduced to sea level using the vertical temperature gradient -0.30°C/100 m a.s.l. The semivariogram estimated from these temperatures is presented in Figure 6.10 together with the semivariogram based on temperatures reduced by the constant lapse rate (Figure 6.1). There are only small differences in the spatial covariance structure. It seems though that the semivariogram based on the constant lapse rate temperatures has a more defined sill and range. In the semivariogram based on the seasonal reduced temperatures, there seems to be a second spatial structure for distances larger than ~200 km. This nested structure indicates variation in the process at different scales. In this case, it can be a signal of different lapse rates in the dataset, and that the separation distance between these processes are approximately 200 km. However, the semivariogram parameters is very similar in the two approaches, and the estimates are most vulnerable for changes in the parameters at short distances. This will change the weights of the closest stations considerably, while applying a large range, including many stations in the estimation, a small change in the variogram parameters will not influence the estimates much.

Cross-validation results by applying the seasonal lapse rate is presented in Figure 6.12. The estimates show generally better fit than the estimates from applying a constant lapse rate. Especially the estimates of temperature at eastern inland stations are improved. This is the area where the vertical temperature gradient often is expected to be positive due to inversions, and thereby increase the average lapse rate. As it can be seen from Figure 6.12, temperatures are still often underestimated at stations located at hillsides compared to stations located at the valley floor. This is an effect of the high weighting given to neighbouring stations in the interpolation routine. A valley station will automatically reduce the temperatures in its surroundings compared stations located higher in the terrain.

The resulting temperature map is shown in Figure 6.13, and shows a more credible map than the map presented in Figure 6.9. The map has a weaker topographical signal, and show a stronger distance from coast dependence. This is in accordance with the results obtained by Tveito (1998).

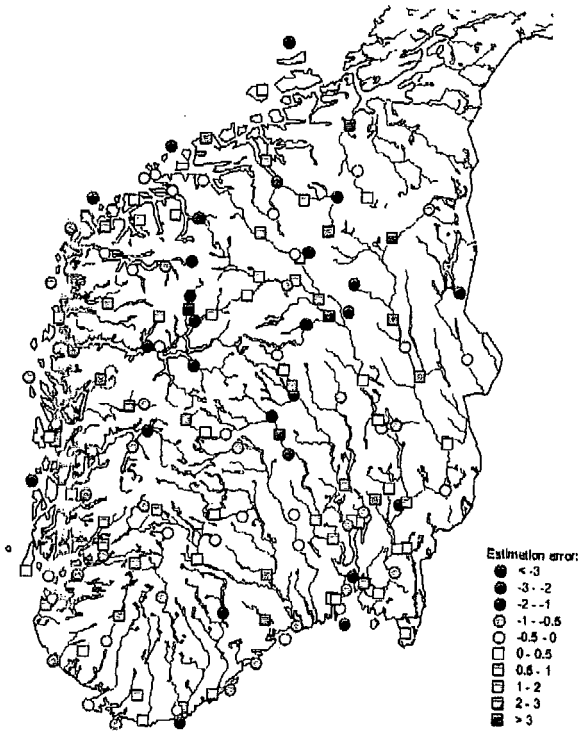

Figure 6.11 Crossvalidation at sea level (seasonal lapse rate), January.

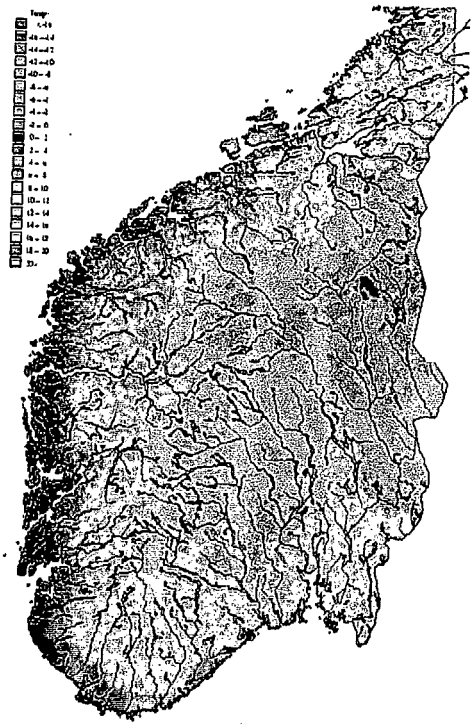

Figure 6.12 Interpolated temperature at terrian level (seasonal lapse rate), January.

7. Uncertainties in the estimates.

In this analysis, a combined approach including a deterministic and a geostatistical model is applied. Both model components will include some estimation uncertainties and errors. In this chapter, the estimation errors are discussed, but no attempt has been made to separate the two uncertainty sources.

7.1 Estimation variance

One advantage by applying a geostatistical approach, is the possibility to study the estimation variance. This estimation variance, $\sigma^2(\mathbf{u})$, is used to find the weights, $\lambda_j(\mathbf{u})$, by minimizing the kriging variance:

$$\sigma^2(\mathbf{u}) = C(0) - \sum_{j=1}^{n} \lambda_j(\mathbf{u}) C(\mathbf{u}_0 - \mathbf{u}_j) \qquad \geq 0$$

This estimation variance can be estimated for any point, and is a good measure for the accuracy of different models. Since the estimation variance is a result of the spatial covariance model, it does not measure the local estimation.

Figure 7.1 shows the estimation variances for January from the two spatial semivariogram models used in this analysis (cf. tables 5.1 and 6.1). The maps show the improvement by the sea level approach compared to the station level approach. This is natural, since the variability is reduced in the sea level approach, and thereby also the semivariogram parameters range and sill. In some areas the estimation variance is large, which tells us that with the present spatial model, the estimate for this area may have a higher uncertainty. However, this measure is a result of the spatial analysis of the observations used, and rely on the information herein. Basically, the estimation variance map indicates where to place new observation stations based on the information from the existing network, and its spatial variance.

The January estimation variance maps have high values compared to the maps for April (Figure 7.2). These maps clearly show the effect by removing the trend (described by the deterministic component) from the non-stationary dataset. The estimation variance map for April temperatures reduced to sea level shows very small variances compared to the station level estimation variances. The small variance at sea level tells us that this approach contains less uncertainty.

7.2 Estimation error.

In a reliable statistical model, the residuals (T - T*) should be the normally distributed $N(\mu,\sigma^2)$, where the mean (μ) should be zero and the variance (σ^2) should be 1.

Figure 7.3 shows the distribution of estimation errors in January as histogram and cumulative Q-Q plot for the estimate the station level approach. The Q-Q plot shows the cumulative distribution of the observations along the x-axis, and the expected distribution if the values follow the normal distribution along the y-axis. Scatter plot of observed vs. estimated temperature is also presented. The shape of the histogram is quite similar to the normal distribution, but the variance is a little high. Regarding the cumulative plot, the distribution of errors shows quite good results, and only one value can be considered as an outlier. This station, 25840 Finse, is located at 1224 m a.s.l., one of the highest altitude levels in the data set. The scatterplot show quite good clustering. It should however be noticed that in Januarythere is a large range of observed, and consequently estimated temperatures.

For the estimated temperatures at sea level (Figure 7.4) applying the constant lapse rate, the results seem to be poorer considering the distribution of errors. The standard deviation is higher, and there are problems specially with to many underestimated values. Considering the scatter of observed vs. estimated temperatures, this plot shows less coherence compared to the station level plot. This may imply problems regarding the validity of the lapse rate used.

For the approach using a seasonal lapse rate for removing the deterministic component of air temperature (Figure 7.5), the results show quite good fit to the normal distribution, however still to many events at the tails.

Looking at the deviations, most of the errors are within a ± 2°C interval, which is very good concerning the large spatial variation of the January surface temperature(-13 to +3 °C).

For estimates at station level in April (Figure 7.6) there are some large errors in the sample. Especially one value may be considered as an outlier (31970, Gaustadtoppen). Generally, low temperatures has not been properly modelled. The fit to the normal distribution is good when considering the large majority of stations. Most of the residuals are within an interval of ±1.5°C.

Applying the constant lapse rate fot the deterministic component results in errors having standard deviation less than 1 (Figure 7.7). The Q-Q plot and the histogram shows quite good approximation to the normal distribution. Most of the residuals are within a ±0.5°C interval. It is worth noticing the small range in observed temperatures (3 to 6 °C) at sea level for this month.

For temperature estimates following interpolation at sea level applying the seasonal lapse rate, the main impression is the same. It should be, since the lapse rate applied is marginally different, and the same spatial model is also applied.

Figure 7.1a Estimation variance January, station level

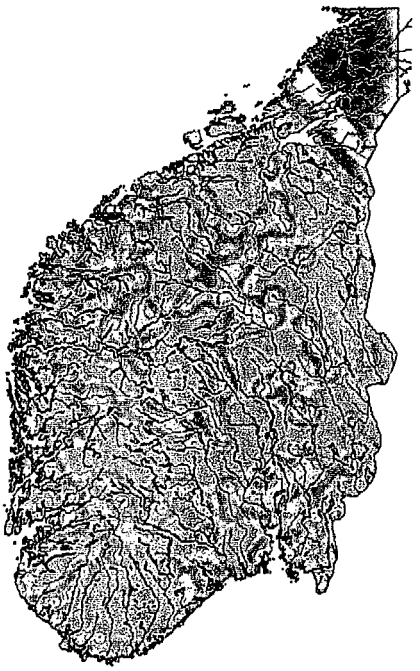

Figure 7.1b Estimations variance in January, sea level

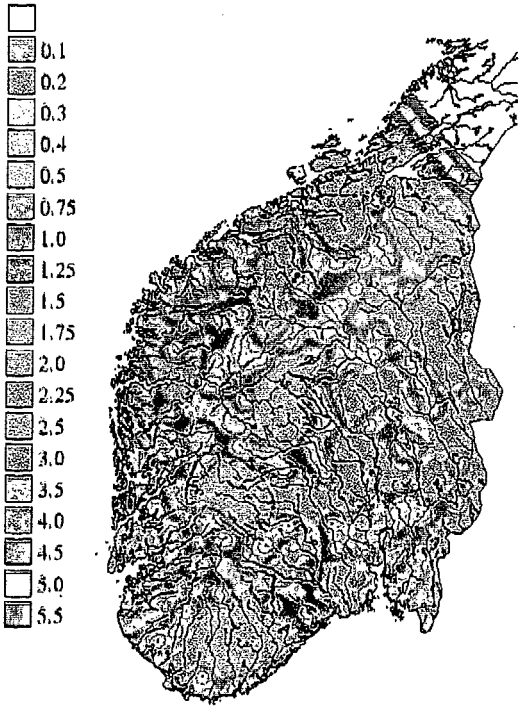

Figure 7.2a Estimation variance in April, station level

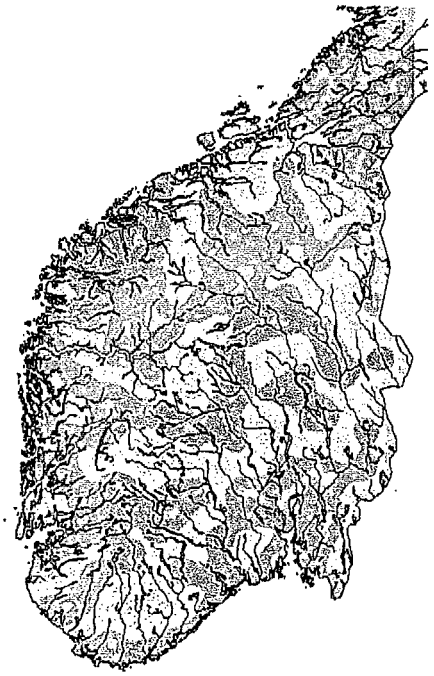

Figure 7.2b Estimation variance in April, sea level

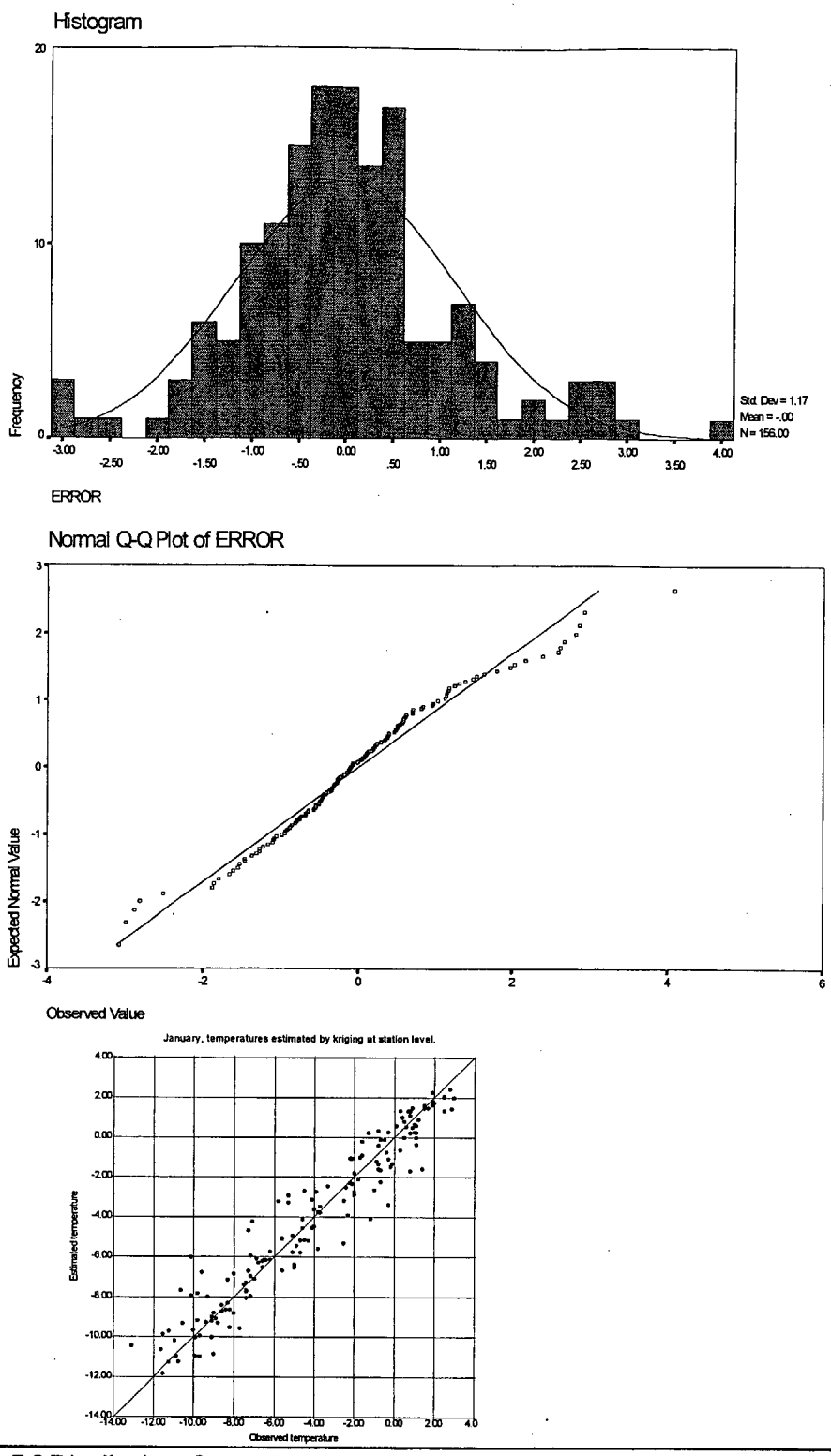

Figure 7.3 Distribution of errors January, station level.

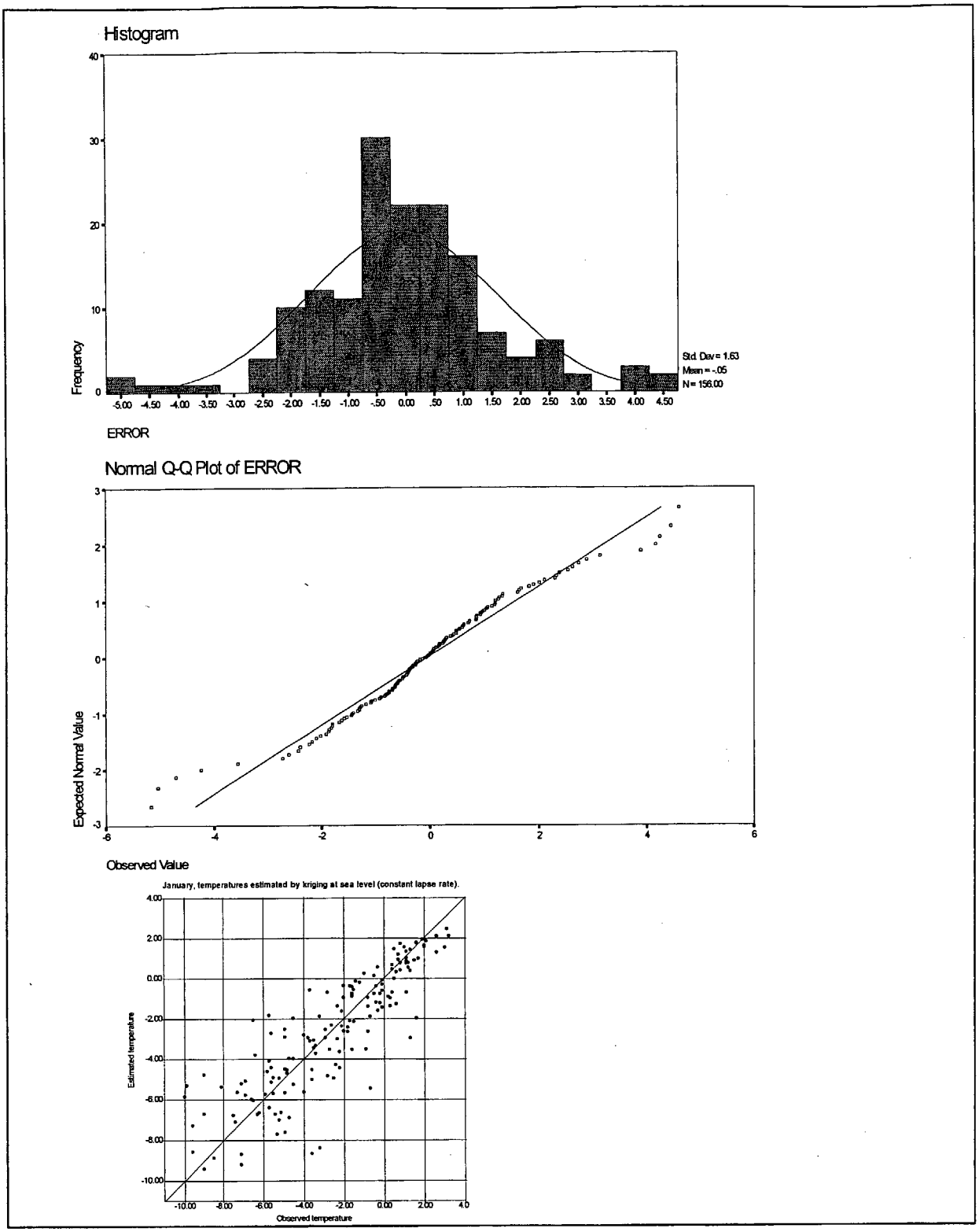

Figure 7.4 Distribution of errors January, sea level constant lapse rate.

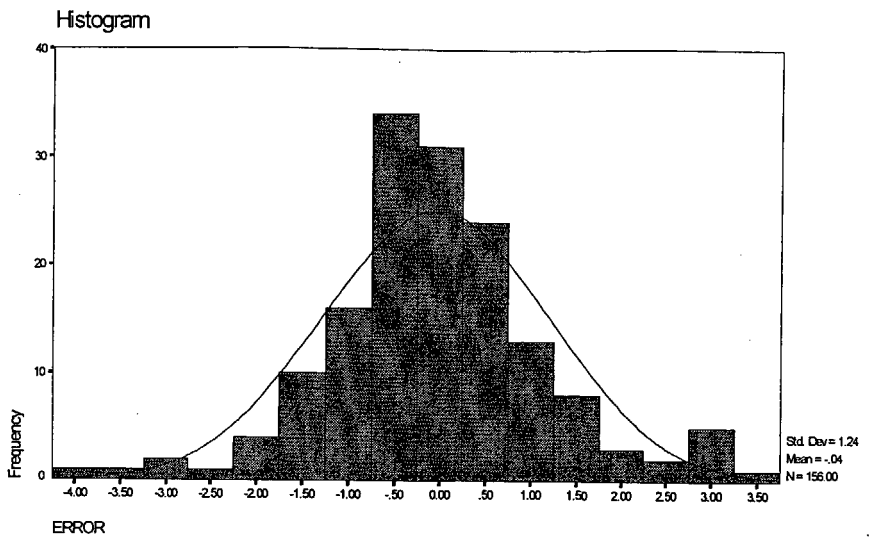

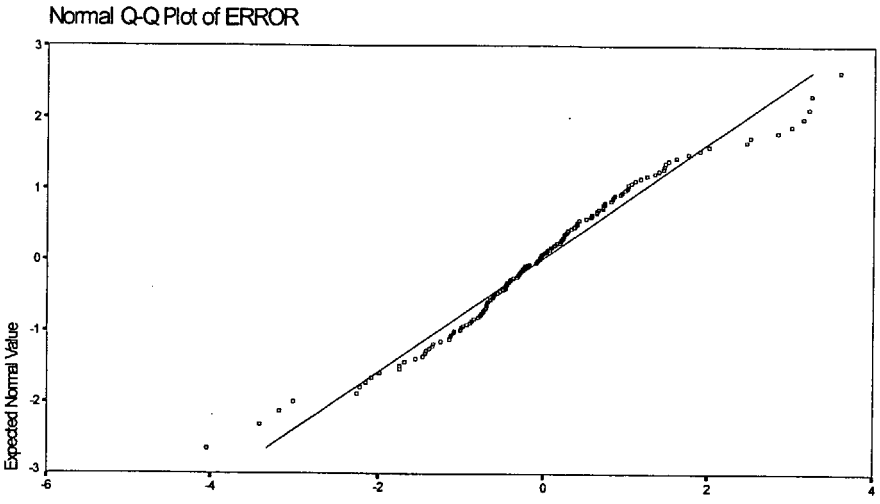

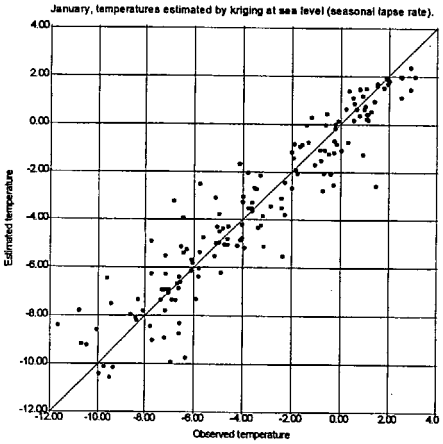

Figure 7.5 Distribution of errors January sea level, seasonal lapse rate.

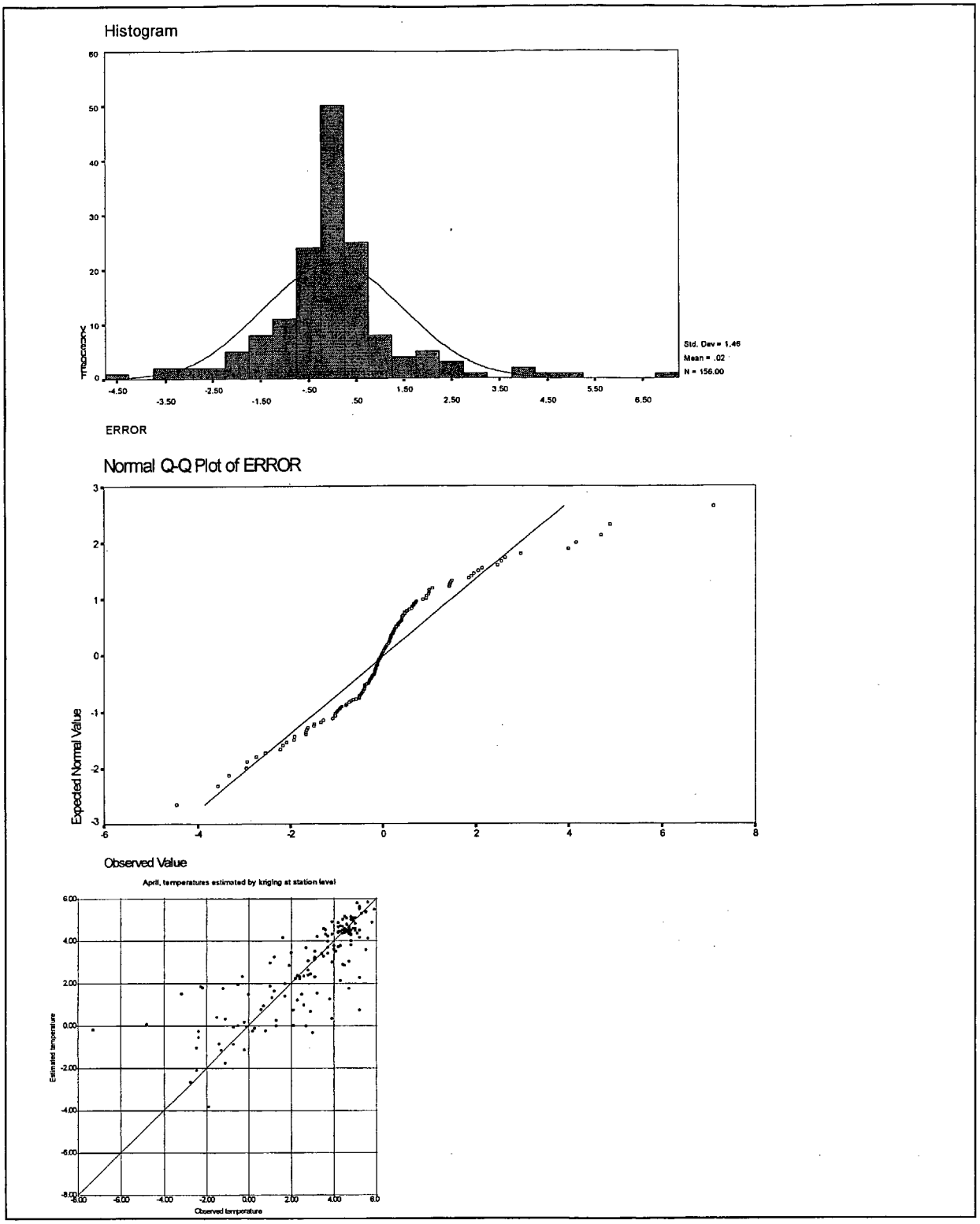

Figure 7.6 Distribution of errors April, station level.

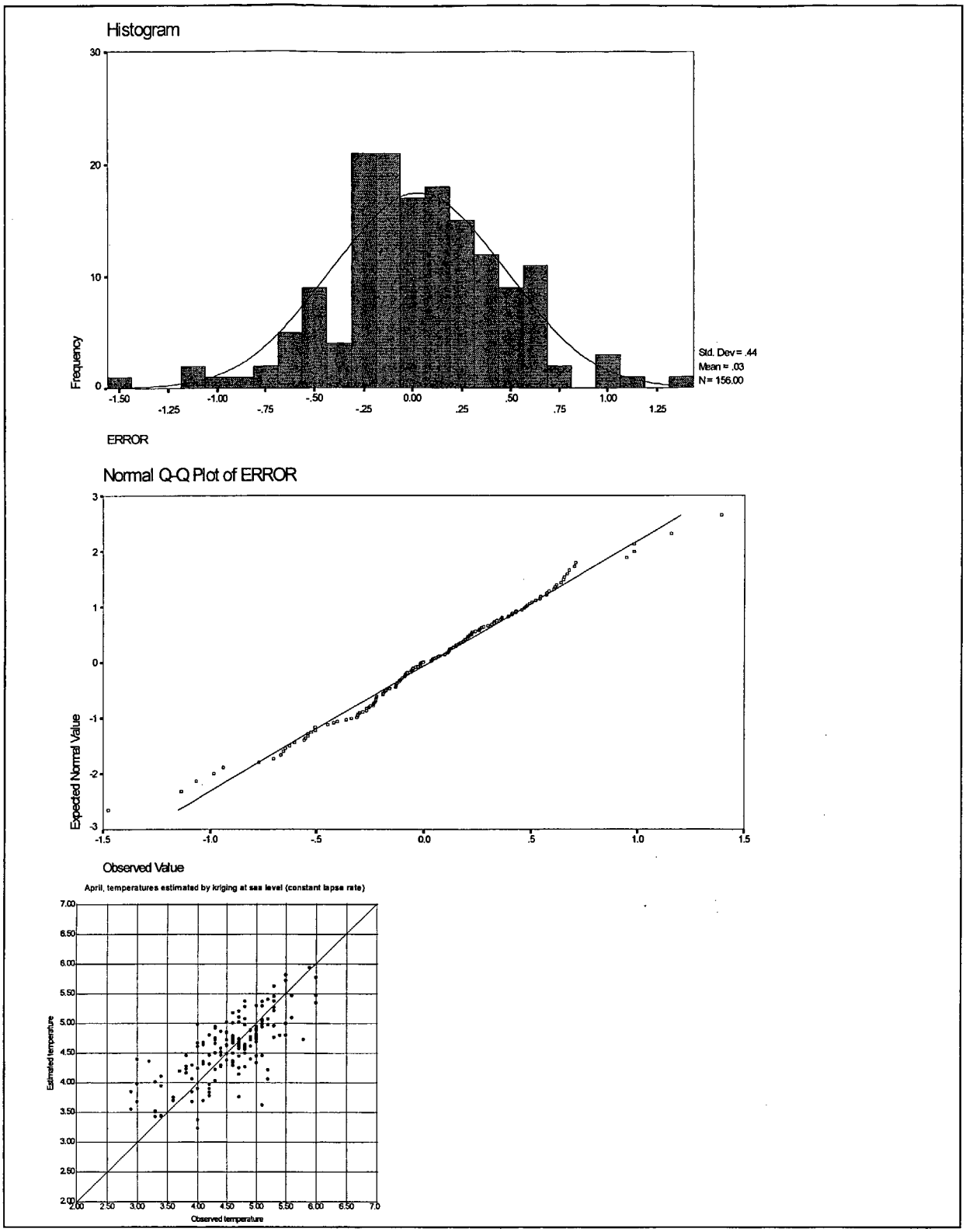

Figure 7.7 Distribution of errors April, sea level constant lapse rate

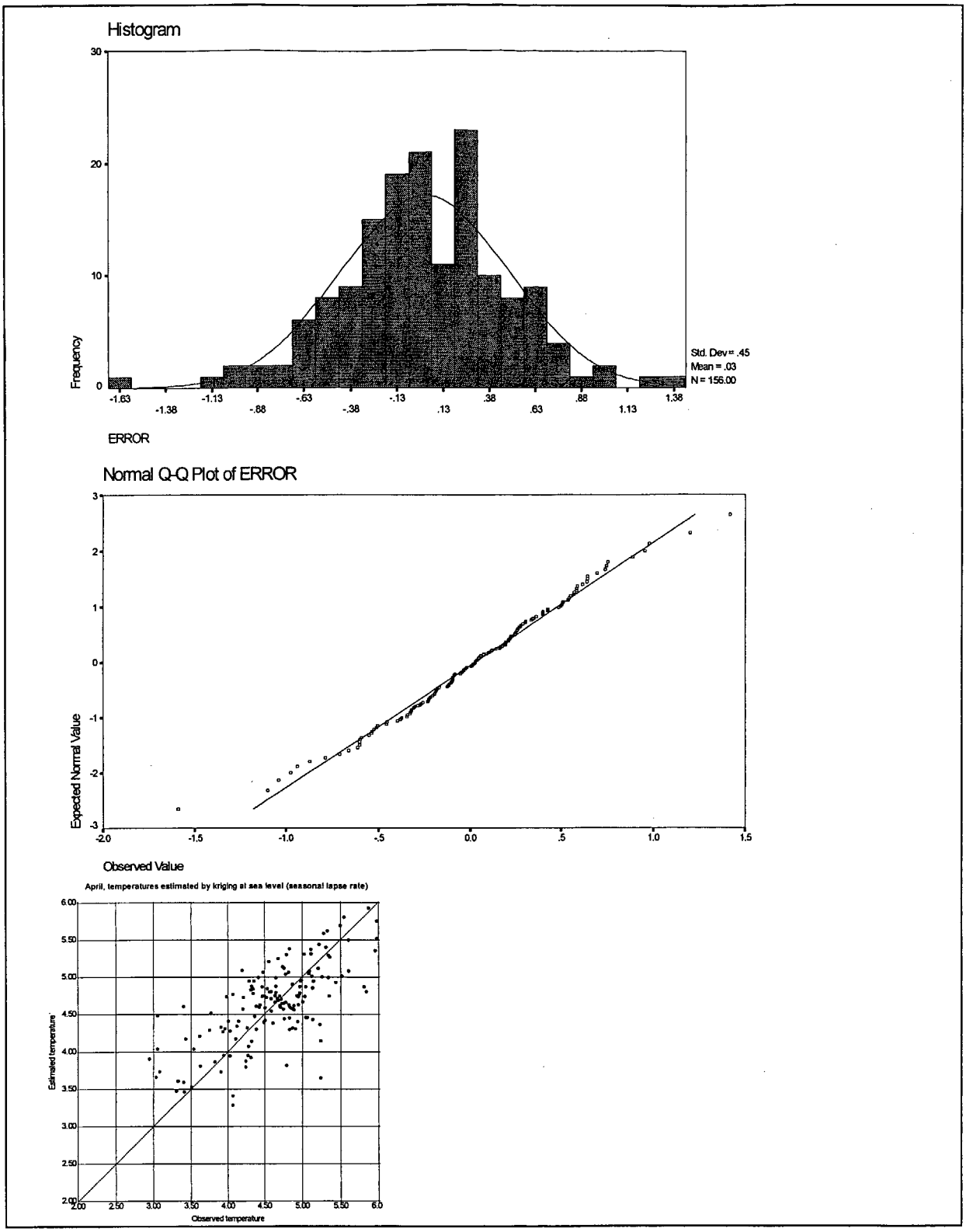

Figure 7.8 Distribution of errors April sea level, seasonal lapse rate

8. Considerations about non-stationarity

So far, the spatial covariance model has been used without checking the validity of the assumptions listed in chapter 2.3.

Knowing the physical and climatological characteristics of temperature, it can be assumed that temperatures are not representing a stationary process. This is verified by Tveito (1998), who shows the relation between the temperature and distance from coast. In order to check the spatial stationarity, directional semivariograms has been computed. A directional semivariogram is based on observations in a certain direction, only regarding observations within a sector defined by a tolerance angle around the principal direction (Figure 8.1). In this investigation, this sector is defined as 20° on both sides from the principal direction. Semivariograms are estimated for all direction in steps of 10° (0°, 10°, 20°....) until all directions are covered. The semivariogram parameters are estimated automatically, taking the sill as ½·Var(·), and range as the shortest distance where $\gamma(h)$ exceeds the sill. The variance is the same for all directions, so any anisotropy is recognised in different ranges. The range is plotted as a function of direction, as shown in Figure 8.2.

In the interpolation routines, an anisotropy factor can be defined. This factor is defined as the ratio between the range in the principal direction, favourably the direction with the longest range, and the range of the direction normal to the principal. In Figure 8.2, this relation is 0.54, and the principal direction is 5°. As seen from Figure 8.2, smoothing has been applied to reduce the influence of single stations deviating from the regional patterns.

This anisotropy factor has been applied on January temperatures reduced to sea level applying the -0.65°C/100 m a.s.l. gradient, and the sea level map and crossvalidation results are presented in Figures 8.3 and 8.4.

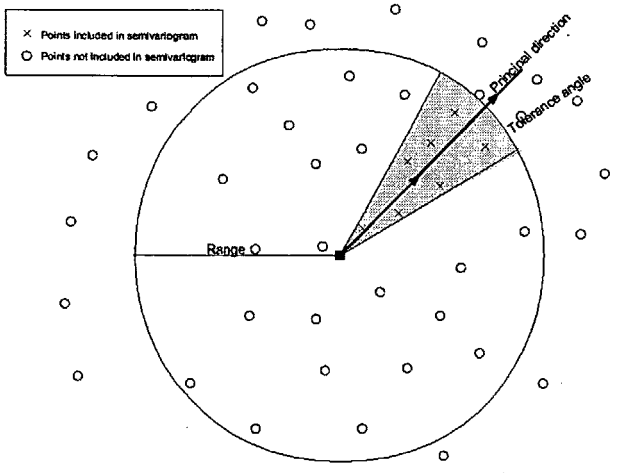

Figure 8.1: Search principles deciding the anisotropy

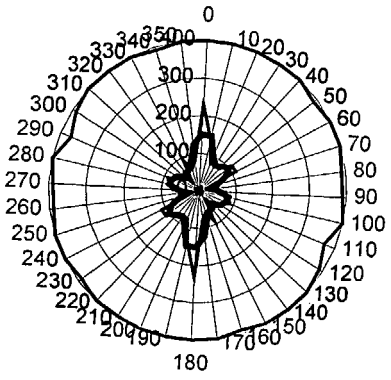

Figure 8.2: Procedure defining the anisotropy factor

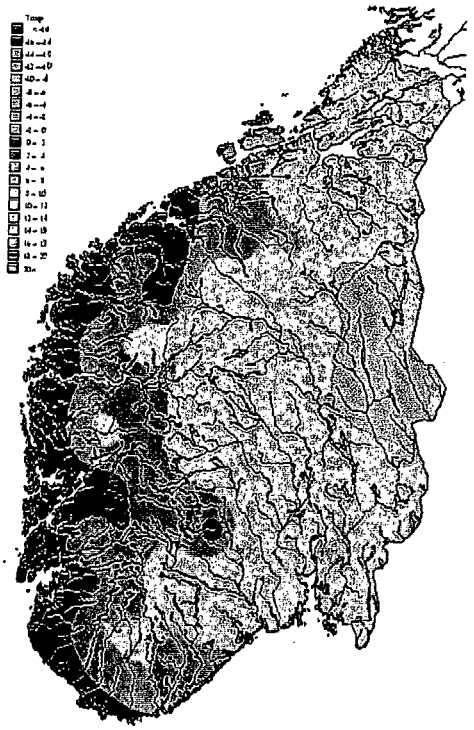

Figure 8.3a: Interpolated temperature at sea level, January, applying an isotropical semivariogram.

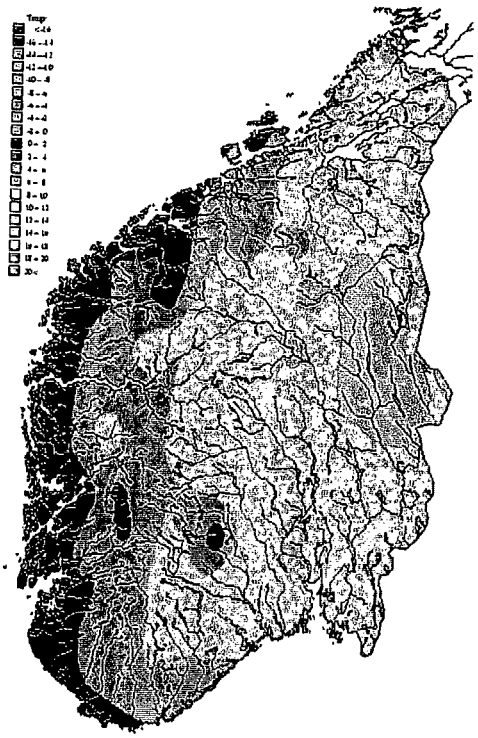

Figure 8.3a: Interpolated temperature at sea level, January, applying an anisotropical semivariogram.

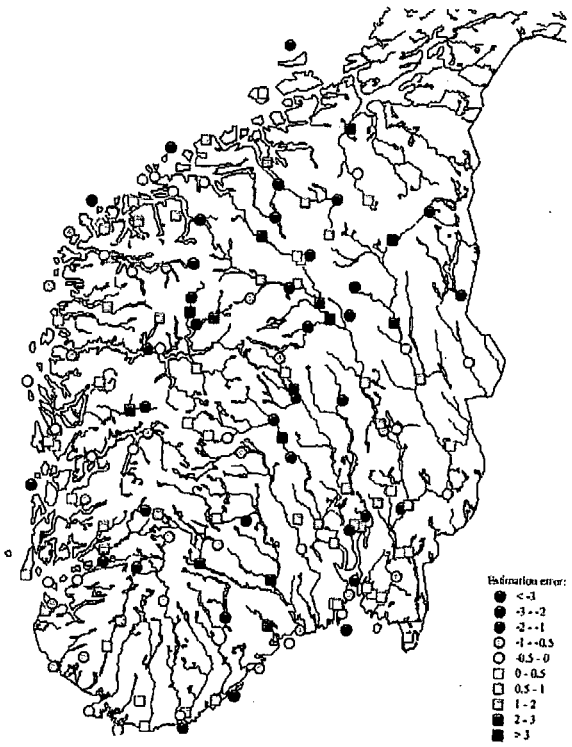

Figure 8.4a: Crossvalidation results applying an isotropical semivariogram at sea level, January.

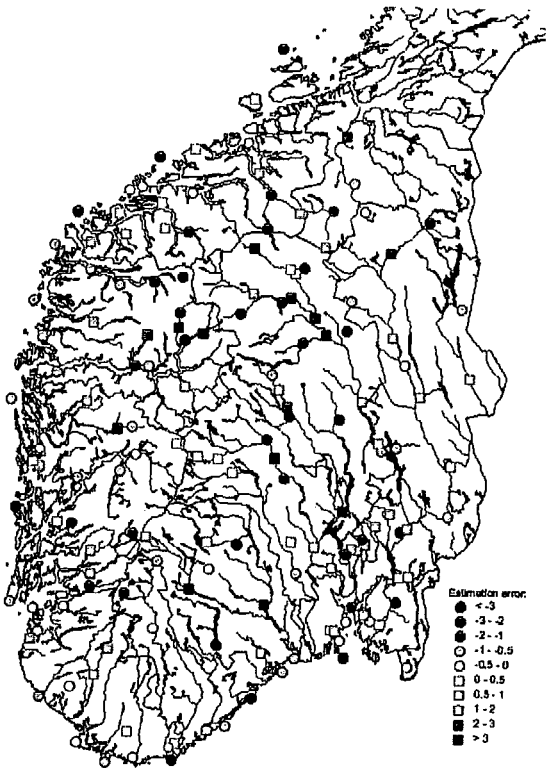

Figure 8.4b: Crossvalidation results applying an anisotropical semivariogram at sea level, January.

9.Conclusions

In this analysis, the spatial variation of mean monthly temperature normals from southern Norway have been studied. An approach combining a deterministic and a geostatistical model has been applied. The deterministic component describes the large scale trend in the temperature, features that have a large scale physical explanation or at least a physical interpretation.

In this study, the deterministic component of temperature is defined as the vertical temperature gradient, the lapse rate. By removing the spatial variability caused by terrain variations, a temperature field more suited for spatial statistical analysis is obtained. The temperatures are reduced to sea level by applying the lapse rate, and kriging is applied for interpolating the residuals. These temperatures are closer to fulfill the assumptions most statistical interpolations methods require, the assumptions about stationarity and isotropy.

Interpolation is done for three different model setups:

1. Interpolation applying kriging without considering the altitude influence, (the station level approach).
2. Interpolation using the global (constant) lapse rate of -0.65°C/100 m a.s.l. as the deterministic model and reduce to temperature at sea level. The reduced temperatures are interpolated applying kriging.
3. As in setup 2, but the seasonal lapse rate obtained by Tveito (1998) is applied as the deterministic component.

For setup 2 and 3, a digitial terrain model is applied to calculate temperatures at terrain level by using the same lapse rate as in the deterministic component.

The results are verified by cross-validation, and both the estimation variance and estimation errors are evaluated. In the study, interpolation of mean normal temperature for January and April is carried out and discussed.

The results are very good, especially for the sea level approach in April. The station level approach for April contains large errors, and supresses the elevation influence. The resulting maps are not reliable.

For January, the temperature shows more variability. The results are also poorer than for April. However, most of the estimates are within a ±2°C deviation from the observed values. The advantage using a deterministic model before performing the spatial interpolation is not as pronouced as for April, probably since the lapse rate is varying in space. Factors like inversions and föhn-winds are influenced by local terrain effects, and use of the mean lapse rate leads to large errors locally. It is easy to see from the results, that stations located at hillsides and at valley floors will be under- respectively overestimated, and that the largest errors occur where stations are close in space, but with a large difference in elevation. Use of a local terrain base instead of reducing the temperatures all the way down to sea level would probably have reduced the errors, and this will be further investigated.

One of the assumptions for applying kriging is that the process is isotropical. Evaluation of directional semivariograms shows that this is not fulfilled for the mean monthly temperature normals for Southern Norway. The anisotropy factor varies throughout the year, and so does the «direction» of the anisotropy. For January, the anisotropy is studied, and it describes the relation between temperature and distance from the sea. A more sophisticated approach using distance to sea as covariate in cokriging, or including it in the deterministic components should be further analysed.

In general, the results show that the methods applied in this study is a major step forward in developing an objective and consistent application for mapping temperature. It is well suited for automatic production of temperature maps integrating the interpolation procedures, the climatological database and GIS.

10.References

Aune,B. (1992) Temperaturnormal, normalperiode 1961-90 (Temperature normals, normal period 1961-90), Reapport 2/93 KLIMA, DNMI

Aune,B. (1993) Nasjonalatlas for Norge, Statens Kartverk

Aune,B. and E.J.Førland (1987) Local climate in the area close to E18 in the Bærum community. Part II: Local temperature conditions (In Norwegian). DNMI-report 22/87 KLIMA, 47pp

Bruun,I. (1957) Lufttemperaturen i Norge 1861-1955, Det norske meteorologiske institutt.

Carrega,P. (1995) A method for the reconstruction of mountain air temperatures with automatic cartographic applications, Theor.Appl.Climatol,52,69-84.

Cressie.N.A.C. (1991) Statistics for spatial data, Wiley

Deutch,C.V. and A.G. Journel (1992) GSLIB - Geostatistical Sofware Library and User's Guide, Oxford University Press.

Førland,E.J. (1984) Lokalklima på Vestlandskysten (Local climate in Western Norway*; in Norwegian)*, Klima 6

Førland, E.J. and A.Skartveit (1979) Radiation balance, energy budget and microclimate in a heathery coastal area (In Norwegian). Lindåsprosjektet, Report No.24, 98pp.

Gandin,L.S. (1963) Objektivnyi analyz meteorologicheskikh polei, Gidrometeoizdat, Leningrad

Johannessen,T.W. (1977) Vær- og klimaforhold (Weather and climate conditions; *in Norwegian*)(in: GjessingJ.(ed.) Norges Geografi), Universitetsforlaget.

Tveito,O.E. (1998) Spatial estimation of mean monthly temperatures by multiple linear regression, DNMI Report 18/98 KLIMA

Utaaker,K. (1963) The local climate of Nes, Hedmark, University of Bergen Skrifter, Norwegian Universities Press.

Zheng,X. and R.E.Basher (1996) Spatial modelling of New Zealand temperature normals, Int.J.Climatol.,16,307-319.

Appendix A

Station map, list and monthly mean temperature for the normal period 1961-90.

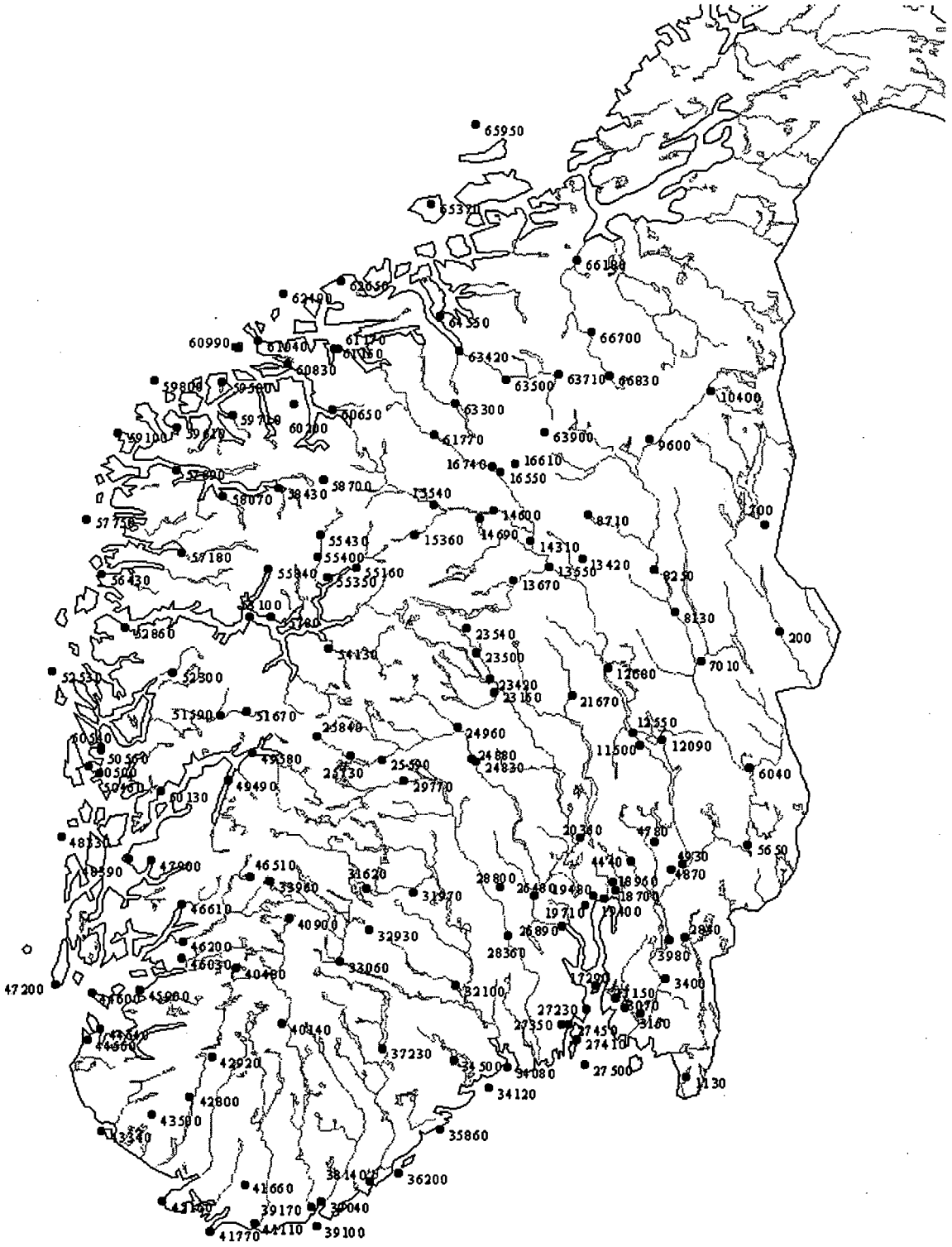

Stnr	Name	Elev	Jan	Feb	Mar	Apr	May	Jun	Jul	Aug	Sep	Oct	Nov	Dec	Ann
200	TRYSIL	356	-10.8	-9.7	-4.7	0.7	7.7	12.7	13.4	12.1	7.6	2.8	-4.2	-9.8	1.5
700	DREVSJØ	672	-11.5	-10.2	-6.3	-1.1	5.5	10.5	11.9	10.6	5.9	1.6	-5.1	-9.6	0.2
1130	PRESTEBAKKE	157	-3.9	-3.6	-0.7	3.6	9.8	14.2	15.7	14.3	10.4	6.6	1.4	-2.4	5.5
2840	HØLAND - KOLLERUD	139	-6.5	-6.0	-1.7	3.1	9.5	14.0	15.0	13.9	9.6	5.6	-0.3	-4.6	4.3
3070	RØD I RÅDE	34	-3.7	-3.5	0.0	4.7	10.5	14.5	16.5	15.4	11.4	7.1	1.8	-1.5	6.1
3150	KALNES	56	-3.8	-3.7	-0.2	4.6	10.4	14.6	16.7	15.6	11.4	7.0	1.8	-1.6	6.1
3400	EIDSBERG	140	-4.5	-4.4	-1.0	4.0	9.6	13.8	15.7	14.5	10.4	6.1	0.8	-3.1	5.2
3980	BÅSTAD	154	-6.2	-6.0	-1.7	3.1	9.6	13.8	14.9	13.8	9.3	5.4	-0.4	-4.5	4.3
4440	HAKADAL - BLIKSRUDHAGAN	174	-6.8	-6.4	-1.8	2.9	9.3	14.1	15.2	13.6	9.2	4.8	-1.3	-6.1	3.9
4780	GARDERMOEN	202	-7.2	-7.1	-2.3	2.8	9.4	14.1	15.2	13.9	9.3	4.7	-1.5	-5.7	3.8
4870	EGNERFJELL	247	-5.6	-5.2	-1.0	3.4	9.7	14.3	15.4	14.3	9.9	5.4	-0.5	-4.2	4.7
4930	HVAM	162	-6.9	-6.6	-1.5	3.5	9.9	14.3	15.3	14.1	9.8	5.2	-1.1	-5.3	4.2
5650	VINGER	175	-7.4	-6.9	-1.8	3.1	9.5	14.2	15.3	13.9	9.5	5.0	-1.4	-6.0	3.9
6040	FLISA	184	-8.6	-7.8	-2.5	2.8	9.4	14.2	15.1	13.7	8.9	4.2	-2.3	-7.1	3.3
7010	RENA - HAUGEDALEN	240	-11.2	-9.6	-3.7	1.7	8.2	13.2	14.3	12.5	7.7	2.9	-4.3	-9.3	1.9
8130	EVENSTAD - ØVERENGET	255	-10.7	-9.6	-3.6	1.7	8.2	13.2	14.3	12.7	8.0	3.0	-4.2	-9.2	2.0
8250	KOPPANG - ØYSET	303	-11.6	-9.5	-4.0	1.3	7.9	12.9	14.0	12.4	7.5	2.6	-4.5	-9.4	1.6
8710	SØRNESSET	739	-9.9	-8.4	-4.8	-0.7	5.2	9.8	11.2	10.3	6.1	2.0	-4.5	-8.2	0.7
9600	TYNSET	483	-13.1	-11.2	-5.7	-0.2	6.3	10.8	12.1	10.8	6.2	1.6	-6.1	-11.0	0.0
10400	RØROS	628	-11.2	-9.7	-5.6	-0.7	5.6	10.1	11.4	10.4	6.1	1.7	-5.2	-9.1	0.3
11500	ØSTRE TOTEN	264	-7.4	-7.0	-2.5	2.3	9.0	13.7	14.8	13.5	9.1	4.6	-1.3	-5.3	3.6
12090	STAUR FORSØKSGÅRD	153	-7.2	-7.6	-2.8	2.6	9.0	13.8	15.1	14.1	9.8	5.2	-0.7	-5.1	3.9
12550	KISE PA HEDMARK	128	-7.4	-8.1	-3.1	2.2	8.5	13.6	15.2	14.0	9.6	5.1	-0.8	-5.3	3.6
12680	LILLEHAMMER - SÆTHERENGEN	239	-9.1	-7.8	-2.8	2.3	8.7	13.5	14.7	13.3	8.5	3.8	-2.6	-7.3	2.9
13420	VENABU	940	-9.7	-9.2	-6.6	-2.3	4.2	9.2	10.4	9.3	4.6	0.3	-5.4	-8.1	-0.3
13550	VINSTRA	241	-11.5	-9.1	-3.3	3.0	9.5	13.9	15.0	13.5	8.3	3.0	-4.5	-9.5	2.4
13670	SKÅBU - STORSLÅEN	890	-9.0	-8.2	-5.4	-1.2	5.0	9.8	11.0	9.9	5.2	1.0	-4.9	-7.4	0.5
14310	OTTA - BREDVANGEN	285	-10.9	-9.3	-3.3	2.6	8.8	13.3	14.5	13.0	8.3	3.4	-4.1	-8.8	2.3
14600	VÅGÅ-KLONES	371	-9.7	-8.6	-3.3	2.1	8.2	12.5	13.9	12.8	8.2	3.5	-3.0	-7.3	2.4
14690	ØVRE TESSA	746	-10.0	-8.9	-5.5	-0.5	5.8	10.3	11.6	10.5	5.5	1.3	-5.0	-8.2	0.6
15360	ELVESETER	674	-9.3	-8.6	-4.5	-0.3	6.1	10.2	11.5	10.3	6.3	2.2	-4.4	-7.4	1.0
15540	GJEILO I SKJÅK	378	-9.4	-8.2	-2.7	2.7	8.5	12.7	13.9	12.8	8.4	3.8	-2.9	-6.6	2.8
16550	DOMBÅS / DOMBÅS II	643	-9.1	-8.0	-4.1	0.2	6.5	10.7	12.0	11.1	6.6	2.2	-4.2	-7.5	1.4
16610	FOKSTUA II	972	-8.8	-8.2	-6.0	-2.4	4.0	8.5	9.8	9.0	4.6	0.9	-4.7	-7.3	0.0
16740	KJØREMSGRENDI	626	-8.9	-7.8	-4.0	0.3	6.5	10.7	12.0	11.1	6.6	2.3	-4.0	-7.3	1.5
17150	RYGGE	40	-4.1	-4.2	-0.4	4.2	10.3	14.7	15.9	14.9	10.8	6.8	1.2	-2.5	5.6
17290	JELØY	12	-2.3	-2.8	0.3	4.6	10.5	15.0	16.6	15.8	11.9	7.8	2.6	-0.8	6.6
18700	OSLO - BLINDERN	94	-4.3	-4.0	-0.2	4.5	10.8	15.2	16.4	15.2	10.8	6.3	0.7	-3.1	5.7
18960	TRYVASSHØGDA II	528	-5.6	-5.3	-2.9	1.6	7.8	12.4	13.6	12.6	8.3	4.1	-1.1	-4.1	3.5
19400	FORNEBU	10	-4.6	-4.5	-0.3	4.8	11.3	15.8	17.1	15.9	11.5	6.7	0.8	-3.2	5.9
19480	DØNSKI	59	-5.1	-5.0	-0.8	4.3	10.8	15.3	16.5	15.1	10.3	5.8	-0.2	-4.2	5.2
19710	ASKER	163	-4.7	-4.6	-0.9	3.5	9.9	14.6	15.9	14.7	10.5	5.9	0.4	-3.2	5.2
20360	EGGEMOEN	192	-8.3	-8.2	-2.5	3.1	9.4	14.3	15.5	13.9	9.0	4.1	-1.8	-6.1	3.5
21670	AUST-TORPA II	485	-8.6	-7.2	-3.3	1.0	7.1	12.0	13.2	11.7	7.3	2.8	-3.4	-7.2	2.1
23160	ÅBJØRSBRÅTEN	639	-9.1	-7.9	-4.8	0.0	5.9	10.7	12.1	11.0	6.6	2.4	-4.1	-7.4	1.3
23420	FAGERNES	365	-10.5	-9.1	-3.9	1.3	7.3	12.4	13.8	12.5	7.9	3.3	-3.8	-8.5	1.9
23500	LØKEN I VOLBU	525	-9.9	-8.4	-4.1	0.8	6.8	11.7	13.1	11.8	7.1	2.7	-4.1	-8.4	1.6
23540	BEITOSTØLEN	822	-9.8	-9.0	-6.2	-1.5	4.5	9.8	11.1	9.9	5.0	1.3	-4.8	-8.0	0.2
24830	AASEN	369	-7.7	-6.2	-1.9	2.4	8.1	12.9	14.1	12.8	8.3	3.8	-2.8	-6.5	3.1
24880	NESBYEN - SKOGLUND	167	-10.1	-8.5	-2.2	3.2	9.1	14.2	15.4	13.7	8.6	3.7	-4.1	-8.6	2.9
24960	GOL - STAKE	542	-8.2	-6.9	-3.4	1.2	7.0	11.8	13.0	11.8	7.2	2.9	-3.3	-6.7	2.2
25590	GEILO - GEILOSTØLEN	810	-8.2	-7.5	-5.2	-1.1	4.7	9.8	11.2	10.2	5.8	2.1	-3.6	-6.5	1.0
25730	HAUGASTØL	988	-9.0	-8.5	-6.8	-2.8	2.9	7.8	9.8	9.2	5.2	1.6	-4.2	-7.3	-0.2
25840	FINSE	1224	-10.1	-9.7	-8.2	-4.8	0.3	5.0	7.0	6.8	3.0	-0.5	-5.6	-8.5	-2.1
26480	BUSKERUD	58	-7.3	-6.3	-1.2	4.0	10.3	15.1	16.3	14.9	10.3	5.4	-1.0	-5.6	4.6

Stnr	Name	Elev	Jan	Feb	Mar	Apr	May	Jun	Jul	Aug	Sep	Oct	Nov	Dec	Ann
26890	DRAMMEN - MARIENLYST	3	-5.6	-5.1	-0.1	4.8	11.0	15.6	16.8	15.5	11.1	6.5	0.2	-4.1	5.6
27230	SLAGENTANGEN	31	-2.5	-2.8	0.4	4.8	10.7	15.2	16.5	15.7	11.6	7.5	2.5	-0.9	6.6
27350	STOKKE	76	-4.0	-4.0	-0.2	4.2	10.4	14.7	15.8	14.6	10.5	6.4	1.1	-2.6	5.6
27410	MÅKERØY	43	-2.4	-2.7	0.4	4.6	10.6	15.3	16.7	15.7	11.8	7.8	2.7	-0.7	6.7
27450	MELSOM	26	-3.7	-3.8	0.0	4.4	10.6	15.0	16.3	15.2	11.1	7.0	1.7	-2.1	6.0
27500	FÆRDER FYR	6	-0.7	-1.5	0.9	4.5	10.0	14.8	16.5	16.2	12.9	9.2	4.6	1.4	7.4
28360	KONGSBERG II / III	171	-6.6	-5.5	-0.9	3.7	9.9	14.8	15.8	14.4	9.8	5.2	-1.3	-5.1	4.5
28800	LYNGDAL I NUMEDAL	288	-7.4	-6.3	-2.0	2.5	8.6	13.4	14.5	13.1	8.6	4.3	-2.1	-6.0	3.4
29770	DAGALI - FAGERLUND	871	-8.4	-7.6	-5.5	-1.4	4.5	9.3	10.7	9.8	5.7	2.1	-4.0	-6.9	0.7
31620	MØSSTRAND II	977	-8.0	-7.9	-5.6	-1.9	3.8	9.4	10.5	9.6	5.6	1.8	-3.2	-6.4	0.6
31970	GAUSTATOPPEN	1828	-10.6	-11.1	-9.9	-7.3	-2.2	2.4	4.2	3.7	0.0	-2.8	-7.8	-9.8	-4.3
32100	GVARV	26	-6.6	-5.8	-0.7	4.3	10.2	14.9	16.0	14.6	10.0	5.6	-0.4	-4.9	4.8
32930	ØYFJELL I TELEMARK	803	-7.0	-6.5	-4.5	-0.5	5.3	10.3	11.4	10.2	6.0	2.5	-2.6	-5.5	1.6
33060	DALEN I TELEMARK II	77	-5.0	-4.7	-0.5	3.9	9.6	14.2	15.6	14.4	10.0	5.5	-0.2	-3.3	5.0
33960	HAUKELISETER BRØYTESTASJON	1019	-8.0	-7.5	-6.0	-2.5	3.5	9.0	10.0	9.0	5.5	1.5	-3.5	-6.0	0.4
34080	LANGØYTANGEN FYR	6	-2.0	-2.1	0.8	4.6	9.8	14.4	16.0	15.6	12.2	8.2	3.2	-0.1	6.7
34120	JOMFRULAND FYR	12	-1.8	-2.1	0.9	4.7	10.3	14.8	16.4	15.7	12.1	8.2	3.3	0.0	6.9
34500	VEFALL I DRANGEDAL	67	-5.3	-4.8	-0.8	3.9	9.9	14.8	16.3	14.9	10.7	6.6	1.1	-3.5	5.3
35860	LYNGØR FYR	4	-0.8	-1.2	1.2	4.8	10.1	14.5	16.2	15.8	12.6	9.0	4.3	1.2	7.3
36200	TORUNGEN FYR	12	-0.3	-0.8	1.3	4.4	9.4	13.7	15.5	15.3	12.5	9.1	4.6	1.6	7.2
37230	TVEITSUND	252	-4.0	-4.8	-0.9	3.2	8.9	13.6	15.1	14.0	9.9	6.0	1.0	-2.0	5.0
38140	LANDVIK	6	-1.6	-1.9	1.0	5.1	10.4	14.7	16.2	15.4	11.8	7.9	3.2	0.2	6.9
39040	KJEVIK	12	-1.7	-1.8	1.0	4.6	9.9	14.0	15.5	14.8	11.5	7.9	3.1	-0.1	6.6
39100	OKSØY FYR	9	0.3	-0.3	1.6	4.5	9.4	13.3	15.2	15.2	12.5	9.3	5.0	2.1	7.3
39170	KRISTIANSAND S	22	-0.9	-1.2	1.6	5.2	10.3	14.2	15.7	14.9	11.7	8.1	3.4	0.5	7.0
40140	HYLESTAD - BROKKE	443	-4.7	-4.4	-1.5	2.1	7.5	11.9	13.3	12.4	8.5	4.9	1.7	-3.4	4.0
40480	SANDDOKKRYGGEN	1105	-7.3	-7.1	-6.1	-3.2	2.4	6.6	8.3	7.9	4.2	0.5	-3.3	-6.1	-0.3
40900	BJÅEN	927	-7.5	-7.7	-5.1	-1.3	4.2	8.7	10.5	9.9	6.0	2.4	-3.0	-6.5	0.9
41110	MANDAL II	138	-0.5	-0.8	1.2	4.6	9.6	13.4	14.8	14.4	11.2	8.0	3.8	1.1	6.7
41660	KONSMO - EIKELAND	260	-2.1	-2.1	0.2	3.6	8.8	12.9	14.2	13.4	9.9	6.6	2.2	-0.7	5.6
41770	LINDESNES FYR	13	1.1	0.5	2.0	4.7	9.0	12.5	14.2	14.8	12.4	9.6	5.6	2.9	7.4
42160	LISTA FYR	14	1.0	0.5	2.2	4.9	9.2	12.4	13.9	14.6	12.2	9.4	5.5	2.7	7.4
42800	TONSTAD	57	-2.0	-2.2	0.8	4.4	9.8	13.4	15.0	14.4	10.7	6.9	2.3	-1.3	6.0
42920	SIRDAL - TJØRHOM	500	-5.3	-5.4	-2.2	1.0	6.6	11.2	12.4	11.5	8.1	4.8	-0.3	-3.7	3.2
43340	NORDRE EIGERØY	63	1.1	0.7	2.3	4.8	9.0	12.1	13.4	14.1	11.7	9.1	5.2	2.7	7.2
43500	UALAND - BJULAND	196	-0.8	-1.0	1.1	4.3	9.3	12.8	13.9	13.6	10.5	7.5	3.3	0.6	6.3
44560	SOLA	7	0.8	0.6	2.7	5.5	9.9	12.8	14.2	14.4	11.7	8.8	4.6	2.2	7.4
44600	RENNESØY - GALTA	19	1.9	1.4	2.7	5.2	9.4	12.4	13.9	14.3	11.8	9.1	5.5	3.2	7.6
44640	STAVANGER	72	1.2	1.1	2.8	5.5	9.9	12.8	14.1	14.4	11.7	8.8	4.8	2.5	7.5
45900	FISTER	1	1.1	0.9	2.9	5.6	10.1	13.1	14.4	14.4	11.6	8.7	4.6	2.4	7.5
46030	ULLADAL - FJELLBERG	382	-2.2	-2.1	-0.4	2.7	8.2	11.3	12.4	12.1	8.7	5.7	1.6	-1.0	4.8
46200	SULDAL - MO	58	-2.1	-2.0	1.2	4.7	10.0	13.3	14.4	13.8	10.3	7.0	2.0	-0.8	6.0
46510	MIDTLÆGER	1079	-6.4	-6.3	-5.1	-2.4	2.9	6.8	8.6	8.4	4.3	1.2	-3.1	-5.2	0.3
46610	SAUDA	5	-2.0	-1.7	1.4	4.8	10.2	13.7	14.9	14.2	10.6	7.1	2.2	-0.7	6.2
47200	SKUDENES II	2	1.9	1.5	2.9	5.2	9.3	12.2	13.6	14.2	11.9	9.3	5.5	3.5	7.6
47900	INDRE MATRE	24	1.1	0.8	2.6	5.8	10.3	13.2	14.2	13.6	10.8	8.0	4.3	2.0	7.2
48330	SLÅTTERØY FYR	15	2.5	2.1	3.1	5.0	8.7	11.5	13.1	13.8	11.9	9.5	5.9	3.8	7.6
48390	UPSANGERVATN	60	0.9	0.7	2.5	5.1	9.8	12.9	14.1	13.9	11.0	8.2	4.2	2.0	7.1
49490	ULLENSVANG FORSØKSGARD	12	-0.2	-0.4	1.7	5.2	10.2	13.8	15.0	14.1	10.5	7.1	3.1	0.9	6.8
49580	EIDFJORD - BU	117	-1.2	-1.4	1.2	4.7	10.1	13.6	14.6	13.8	10.0	6.6	2.2	0.1	6.2
50130	OMASTRAND	2	0.8	0.6	2.4	5.3	10.3	13.7	14.8	14.3	10.9	8.0	4.0	1.7	7.2
50460	FANA FORSØKSSTASJON	48	0.4	0.2	2.2	4.8	9.6	12.4	13.6	13.4	10.6	7.9	3.8	1.7	6.7
50500	FLESLAND	48	0.8	0.7	2.3	4.8	9.3	12.1	13.3	13.3	10.6	8.0	3.9	1.8	6.7
50540	BERGEN - FLORIDA	12	1.5	1.6	3.3	5.9	10.5	13.5	14.5	14.4	11.5	8.7	4.7	2.6	7.7
50560	BERGEN - FREDRIKSBERG	41	1.7	1.6	3.2	5.6	10.1	12.9	14.0	14.0	11.4	8.7	4.7	2.7	7.6
51590	VOSS - BØ	125	-4.5	-3.8	0.2	3.9	9.3	13.2	14.2	13.4	9.4	5.8	0.3	-3.0	4.9

Stnr Name	Elev	Jan	Feb	Mar	Apr	May	Jun	Jul	Aug	Sep	Oct	Nov	Dec	Ann
51670 REIMEGREND	590	-4.6	-4.2	-1.9	1.2	6.8	10.6	11.8	11.2	7.5	4.3	-0.9	-3.6	3.2
52300 MODALEN	104	-2.2	-2.3	0.6	3.6	8.9	12.5	13.6	13.2	9.5	6.4	1.6	-0.9	5.4
52530 HELLISØY FYR	20	2.5	2.1	3.0	4.9	8.5	11.0	12.8	13.4	11.4	9.1	5.6	3.7	7.3
52860 TAKLE	38	1.0	0.8	2.3	4.7	9.3	12.3	13.5	13.4	10.3	7.8	4.0	2.1	6.8
53100 VANGSNES	51	-0.1	0.2	1.8	5.0	10.0	13.5	14.5	14.1	10.3	7.1	3.2	1.0	6.7
54130 LÆRDAL - TØNJUM	36	-2.5	-2.2	1.3	5.2	10.3	13.6	14.7	13.9	9.9	6.1	1.4	-1.2	5.9
55160 FORTUN	27	-5.1	-4.9	-1.0	3.8	9.6	13.0	14.2	13.2	8.9	4.8	-0.4	-3.4	4.4
55350 LUSTER SANATORIUM	484	-3.8	-3.9	-1.6	2.0	7.5	11.5	12.6	12.0	7.9	4.4	-0.5	-3.0	3.8
55400 MYKLEMYR	98	-7.1	-6.9	-2.5	2.4	8.7	12.9	14.0	12.9	8.6	4.5	-1.6	-5.3	3.4
55430 BJØRKEHAUG I JOSTEDAL	324	-4.9	-4.6	-1.9	1.9	8.0	12.3	13.4	12.5	8.2	4.4	-1.1	-3.8	3.7
55780 LEIKANGER	53	-0.8	-0.5	1.6	5.0	10.3	13.8	14.9	14.2	10.3	7.0	2.6	0.3	6.6
55840 FJÆRLAND - SKARESTAD	10	-3.3	-3.0	-0.1	3.7	9.6	13.3	14.3	13.3	9.3	5.7	0.6	-2.1	5.1
56430 FURENESET	14	1.5	1.2	2.7	5.0	9.3	12.0	13.2	13.2	10.5	8.0	4.5	2.5	7.0
57180 FØRDE I SUNNFJORD II	41	-1.3	-0.6	1.8	4.6	9.6	12.6	13.8	13.6	10.2	7.1	2.3	-0.1	6.1
57750 KINN	10	2.5	2.3	3.1	4.9	8.7	11.0	12.5	13.3	11.2	9.0	5.5	3.6	7.3
57890 DOMBESTEIN	33	0.9	0.8	2.2	4.6	9.3	12.3	13.6	13.5	10.1	7.7	3.6	1.8	6.7
58070 SANDANE	51	-0.4	-0.5	1.7	4.7	9.8	12.8	14.2	13.8	10.0	6.9	2.3	0.2	6.3
58430 OLDEN - VANGBERG	78	-0.7	-1.2	1.2	4.2	9.6	12.8	13.7	13.0	9.2	6.4	2.2	0.0	5.9
58700 OPPSTRYN	201	-1.0	-1.0	0.9	3.7	9.2	12.4	13.5	12.9	9.4	6.5	2.1	-0.2	5.7
59100 KRÅKENES FYR	41	2.8	2.6	3.2	4.7	8.2	10.8	12.6	13.0	11.1	9.0	5.5	3.8	7.3
59580 HAREID - GRIMSTAD	30	0.5	0.7	2.2	4.5	8.9	11.6	13.0	13.0	10.2	7.8	3.5	1.6	6.5
59610 FISKÅBYGD	41	0.7	0.8	2.2	4.7	9.0	11.7	13.0	13.1	10.1	7.7	3.5	1.6	6.5
59710 ØRSTAVIK - VELLE	35	-0.7	-0.3	1.9	4.3	9.2	12.0	13.3	13.2	9.9	7.2	2.3	0.2	6.0
59800 SVINØY FYR	38	3.0	2.7	3.2	4.4	7.5	10.1	11.9	12.7	10.9	9.0	5.7	3.9	7.1
60200 STRANDA - HELSEM	84	-0.8	-0.5	1.7	4.2	9.1	12.2	13.4	13.1	9.8	6.8	2.0	0.2	5.9
60650 VALLDAL - LINGE	50	0.8	1.0	2.9	5.5	10.2	13.0	14.3	13.9	10.6	7.9	3.7	1.5	7.1
60830 SKODJE	26	0.6	0.8	2.3	4.5	9.2	11.9	13.1	13.3	10.2	7.6	3.3	1.4	6.5
60990 VIGRA	22	1.9	1.9	2.8	4.6	8.4	11.0	12.5	13.0	10.6	8.4	4.6	2.8	6.9
61040 HILDRE	13	2.0	1.7	2.8	4.5	8.2	10.9	12.5	12.8	10.7	8.5	4.6	3.0	6.9
61150 GJERMUNDNES	49	0.1	0.5	2.0	4.4	9.0	11.8	13.0	13.2	9.8	7.1	3.1	1.2	6.3
61170 HJELVIK I ROMSDAL	21	0.5	0.7	2.1	4.5	9.1	11.9	13.1	13.2	9.8	7.4	3.3	1.6	6.4
61770 LESJASKOG	621	-9.6	-8.4	-4.4	-0.2	6.1	10.1	11.3	10.6	6.2	2.2	-4.5	-8.2	0.9
62490 ONA - HUSØY	8	2.9	2.8	3.3	4.7	7.8	10.4	12.2	12.8	10.9	9.0	5.6	3.8	7.2
62650 HUSTAD II	26	0.3	0.4	2.0	4.2	8.4	11.1	12.4	12.7	10.0	7.6	3.3	1.4	6.2
63300 AURSJØEN	869	-7.2	-7.1	-5.0	-2.2	3.5	7.6	9.2	9.2	5.6	2.3	-2.9	-5.9	0.6
63420 SUNNDALSØRA III	6	-0.3	0.0	2.2	5.2	10.4	13.2	14.0	13.6	10.5	7.8	3.0	0.9	6.7
63500 SUNNDAL	195	-4.1	-3.6	-0.4	2.9	8.9	12.3	13.3	12.8	8.8	5.3	-0.4	-2.9	4.4
63710 OPPDAL - BJØRKE	625	-5.0	-4.2	-2.4	0.6	6.5	10.0	11.4	10.8	7.1	3.9	-1.5	-3.8	2.8
63900 KONGSVOLL	885	-9.8	-9.5	-6.5	-2.5	4.3	8.9	9.9	8.7	4.6	1.4	-5.4	-8.0	-0.3
64550 TINGVOLL - HANEM	69	-1.6	-1.3	1.1	3.9	9.2	12.3	13.6	13.3	9.5	6.3	1.6	-0.4	5.6
65370 SMØLA - MOLDSTAD	30	-0.3	-0.1	1.3	3.7	8.1	10.8	12.3	12.8	9.6	6.9	2.7	0.9	5.7
65950 SULA FYR	28	1.4	1.6	2.5	4.1	7.5	10.0	11.9	12.3	10.2	8.0	4.4	2.6	6.4
66180 ORKDAL - ØYUM	22	-5.8	-4.9	-1.8	2.8	9.0	12.5	13.6	12.9	8.7	4.5	-1.4	-4.1	3.8
66700 BERKÅK	424	-6.2	-4.7	-2.5	1.1	6.8	11.0	11.9	11.2	7.1	3.6	-2.5	-5.3	2.6
66830 SÆTER I KVIKNE	543	-8.3	-7.4	-4.2	-0.1	5.9	10.1	11.4	10.5	6.5	2.6	-3.6	-6.6	1.4